© 2015. Published by The Company of Biologists Ltd | Development (2015) 142, 3500-3511 doi:10.1242/dev.122564

RESEARCH ARTICLE

STEM CELLS AND REGENERATION

Trithorax regulates systemic signaling during *Drosophila* imaginal disc regeneration

Andrea Skinner, Sumbul Jawed Khan and Rachel K. Smith-Bolton*

ABSTRACT

Although tissue regeneration has been studied in a variety of organisms, from Hydra to humans, many of the genes that regulate the ability of each animal to regenerate remain unknown. The larval imaginal discs of the genetically tractable model organism *Drosophila melanogaster* have complex patterning, well-characterized development and a high regenerative capacity, and are thus an excellent model system for studying mechanisms that regulate regeneration. To identify genes that are important for wound healing and tissue repair, we have carried out a genetic screen for mutations that impair regeneration in the wing imaginal disc. Through this screen we identified the chromatin-modification gene *trithorax* as a key regeneration gene. Here we show that animals heterozygous for *trithorax* are unable to maintain activation of a developmental checkpoint that allows regeneration to occur. This defect is likely to be caused by abnormally high expression of *puckered*, a negative regulator of Jun N-terminal kinase (JNK) signaling, at the wound site. Insufficient JNK signaling leads to insufficient expression of an insulin-like peptide, dILP8, which is required for the developmental checkpoint. Thus, *trithorax* regulates regeneration signaling and capacity.

KEY WORDS: Chromatin, Regeneration, JNK signaling

INTRODUCTION

Regeneration is a complex process through which an organism replaces damaged or lost tissue. Although planarian flatworms and freshwater Hydra are capable of replacing a complete organism (Elliott and Sánchez Alvarado, 2013; Galliot, 2012) and urodele amphibians and teleost fish can replace whole appendages (Gemberling et al., 2013; McCusker and Gardiner, 2011), the regenerative capacity of mammals is restricted and decreases significantly with maturity and age. Therefore, understanding the regulatory mechanisms that permit and promote regeneration in model organisms is of great importance to the field of regenerative medicine, which seeks to enhance the regenerative capacity of human tissues.

Recent work in different model systems has begun to identify the genes and signal transduction pathways that control regeneration. However, it is not clear how tissue damage leads to the activation of these signals and expression of regeneration genes. Interestingly, specific chromatin modifiers are important for regeneration in several organisms, suggesting that chromatin modification regulates the expression of at least some regeneration genes. For example, pharmacological inhibition of histone deacetylases blocks *Xenopus* tail regeneration (Tseng et al., 2011), the H3K27me3 demethylase Kdm6b.1 is required for zebrafish fin regeneration (Stewart et al., 2009), the PRC1 component Bmi1 is required for a regenerative response to pancreatitis in mice (Fukuda et al., 2012), several members of the Set1/MLL family of histone methyltransferases are required for the stem cell-based regeneration that occurs in planaria (Hubert et al., 2014), the SWI/SNF component Brg1 (Smarca4 – Mouse Genome Informatics) is essential for mouse epidermal wound repair and hair regeneration (Xiong et al., 2013) and its *Drosophila* homolog, Brahma, is important for midgut regeneration (Jin et al., 2013). In most of these cases, however, the extent to which tissue damage induces chromatin modification and the genes regulated by these chromatin modifiers during regeneration remain unknown.

Drosophila melanogaster imaginal discs undergo wound repair and regenerative growth, replacing lost tissue and patterning (reviewed by Worley et al., 2012). These tissues are an excellent system for studying regeneration because they are a simple columnar epithelium, but they have complex patterning and fate determination that have been well characterized. Furthermore, the genetic tractability of *Drosophila* and plethora of available reagents are an advantage over many vertebrate models of regeneration. The recent development of genetic tools that induce tissue ablation and allow regeneration to occur *in situ* has enabled analysis of the complex signaling and patterning events that occur during imaginal disc repair (Bergantiños et al., 2010; Smith-Bolton et al., 2009). Here, we used these tools to identify the chromatin-modification gene *trithorax* (*trx*) (Breen and Harte, 1991; Kuzin et al., 1994) in an unbiased forward genetic screen for genes important for imaginal disc regeneration.

By analyzing regeneration in imaginal discs with reduced levels of Trx, we demonstrate that mutant damaged tissue failed to express sufficient levels of the insulin-like peptide dILP8, which delays entry into metamorphosis to allow time for regeneration to occur (Colombani et al., 2012; Garelli et al., 2012). We propose a model in which Trx is important for ensuring proper levels of Jun N-terminal kinase (JNK) signaling after tissue damage, which in turn induces expression of *dilp8* (*Ilp8* – FlyBase). This identification of a mechanism through which one chromatin modifier regulates the local and systemic response to wounding confirms a role for epigenetic regulation of regeneration and opens the door for further identification of regeneration genes.

RESULTS

Tissue heterozygous for *trithorax* regenerates poorly

To enable large-scale regeneration experiments and forward genetic screens, we use genetic tools to induce tissue damage and regeneration in the developing *Drosophila* wing imaginal disc (Smith-Bolton et al., 2009). By using *rotund* (*rn*)-*GAL4* and *tubulin-GAL80^{ts}* to regulate expression of the pro-apoptotic gene

Department of Cell and Developmental Biology, University of Illinois Urbana-Champaign, Urbana, IL 61853, USA.

*Author for correspondence (rsbolton@illinois.edu)

Received 23 January 2015; Accepted 1 September 2015

Development (2015) 142, 3500-3511 doi:10.1242/dev.122564

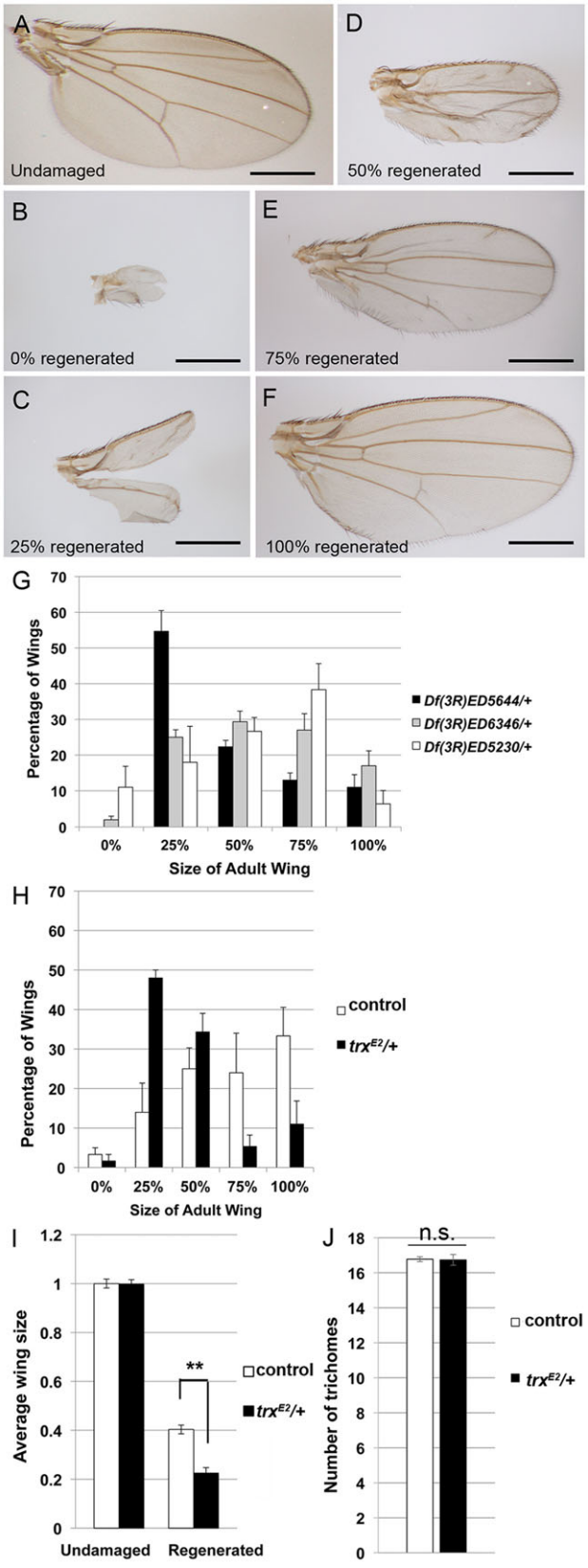

Fig. 1. Reduction of *trx* impairs regeneration. (A-F) Examples of adult wings after regeneration: (A) undamaged; (B) 0%; (C) 25%; (D) 50%; (E) 75%; and (F) 100%. Scale bars: 0.5 mm. (G,H) Ablation and regeneration were induced in the wing imaginal discs. Adult wings were sorted by size to quantify the extent of regeneration. (G) Animals heterozygous for *Df(3R)ED5644* (n=146 wings) had smaller wings than animals heterozygous for *Df(3R)ED6346* (n=94 wings) or *Df(3R)ED5230* (n=42 wings). n is cumulative for three experiments. Distributions are significantly different; χ^2 test P<0.0001. (H) Animals heterozygous for trx^{E2} (n=76) had smaller wings than control animals (n=241). n is cumulative for three experiments. Distributions are significantly different; χ^2 test P<0.0001. (I) Wing area normalized to the average size of 34 control undamaged wings. trx^{E2}/+ undamaged n=33, control regenerated n=216 and trx^{E2}/+ regenerated n=93. Samples included male and female wings. $^{**}P<2\times10^{-7}$. (J) Number of trichomes in a 50×50 pixel box. trx^{E2}/+ regenerated wings (n=27) had cells no different in size from those in control regenerated wings (n=94). Average of wings from three experiments. All error bars are s.e.m. n.s., not significant.

UAS-reaper, most of the wing pouch (>94%) can be ablated in a spatially and temporally defined manner in hundreds of third instar larvae simultaneously (Smith-Bolton et al., 2009). Briefly, the animals are maintained at 18°C until 7 days after egg laying, which is early third instar. The vials are then placed in a 30°C circulating water bath for 24 h before rapidly cooling to 18°C in an ice-water bath to halt expression of UAS-*reaper* and returning to an 18°C incubator. The 24 h induction of *UAS-reaper* is sufficient for almost complete ablation of the *rn*-expressing cells. After ablation, the wing pouch regrows and re-patterns, producing an adult wing upon metamorphosis. Measuring the adult wing size provides a quantification of the extent of regenerative growth (Fig. 1A-F). Measuring a large population of wings determines the average amount of regenerative growth for a specific genetic background.

Using this system, we designed an unbiased forward genetic screen to identify novel and unpredicted regeneration genes that regulate all steps of regeneration, including wound closure, blastema formation, growth, repatterning and the whole-animal developmental arrest that occurs during imaginal disc regeneration. To identify loci that regulate regeneration, screening conditions were established such that discs in most lines in an isogenic collection of mutations regenerated a moderate amount, producing wings that were smaller than undamaged wings (Fig. 1G; Smith-Bolton et al., 2009). Mutations that led to a consistent increase or decrease in average regenerated wing size could then be isolated. Two pilot dominant-modifier genetic screens (Smith-Bolton et al., 2009) that used isogenic deficiencies (Ryder et al., 2007) and a collection of growth-control mutants in an isogenic background (Tapon et al., 2002) successfully identified mutations that impaired or promoted tissue regeneration.

These initial screens isolated a deficiency, *Df(3R)ED5644*, that impaired regeneration as assessed by adult wing size when compared with other isogenic deficiencies (Smith-Bolton et al., 2009; Fig. 1G). In screening conditions, most adult wings from damaged and regenerated *Df(3R)ED5644*/+ wing discs were 25% the size of a normal wing, whereas isogenic deficiencies that did not impact regeneration resulted in adult wings that were most often ≥50% the size of a normal wing (Fig. 1G; Smith-Bolton et al., 2009).

To identify the gene responsible for the *Df(3R)ED5644*/+ phenotype, we tested smaller deficiencies and mutations in candidate genes within the region, including *trx* and *suppressor of Hairy wing* [*su(Hw)*]. As an additional control in all experiments, we compared regeneration in these mutant lines with regeneration in the commonly used control line w^{1118} (Hazelrigg et al., 1984), because it was comparable to the isogenic deficiencies that did not impact regeneration in our pilot screen (data not shown). A strong hypomorphic allele of *trx*, trx^{E2} (Kennison and Tamkun, 1988), consistently regenerated worse than w^{1118} (Fig. 1H; Fig. S1A).

To confirm our semi-quantitative screen findings, we imaged all wings and calculated the area per wing to quantify the difference in

Development (2015) 142, 3500-3511 doi:10.1242/dev.122564

size between trx^{E2}/+ and control regenerated wings (Fig. 1I). To determine whether the difference in size was the result of fewer cells or smaller cells, we calculated cell density by counting the actin-rich trichomes that protrude from one vertex of each cell. Cell density was not different between the control and the mutant (Fig. 1J). To confirm that the poor regeneration phenotype observed in the trx^{E2}/+ mutants was indeed the result of a reduction in Trx levels, we used RNAi to knock down *trx* in the *rn*-expressing cells that survived ablation. We used two independently generated RNAi transgenes targeting *trx*: JF01557 from the Transgenic RNAi Project (TRiP) collection (Ni et al., 2009), which we used in conjunction with *UASdicer2* as recommended, and KK108122 from the Vienna *Drosophila* Resource Center (VDRC) (Dietzl et al., 2007), which has been confirmed to knock down *trx* in imaginal wing discs (Mohan et al., 2011). Expression of either RNAi in the subset of blastema cells that expressed *rn* yet survived ablation impaired regeneration (Fig. S1B,C).

Tissue damage does not cause global deregulation of epigenetically regulated gene expression

Trx acts in the TAC1 complex to methylate Lysine 4 of Histone 3 (H3K4) and is required for the expression of homeotic genes during development (reviewed by Grimaud et al., 2006). Although Trx has been linked to H3K4 trimethylation, most H3K4 trimethylation is carried out by *set1*, with some contribution by *trithorax related* (*trr*) (Ardehali et al., 2011; Hallson et al., 2012). Loss of *trx* does not lead to a visible decrease in H3K4me3 levels in imaginal discs (Kanda et al., 2013). Indeed, recent work has suggested that Trx is a monomethyltransferase (Tie et al., 2014).

There are two possible explanations for the poor regeneration in trx^{E2}/+ animals. Regeneration might require a global relaxation of chromatin-mediated gene silencing, as is thought to underlie the aberrant cell fate changes called transdetermination that can follow tissue damage (Lee et al., 2005). Alternatively, chromatin changes might occur only at specific genes that must be induced or silenced to facilitate regeneration, as can occur during developmental patterning and growth control (Classen et al., 2009; Oktaba et al., 2008). Indeed, chromatin remodeling regulates specific regeneration genes after tissue damage, including *notch1* and *bmp2* in *Xenopus* tails, *Shh* in mouse skin and *dlx4a* in zebrafish fins (Stewart et al., 2009; Tseng et al., 2011; Xiong et al., 2013).

To distinguish between these possibilities, we examined expression of *ultrabithorax* (*ubx*), which is normally expressed in the haltere and third thoracic leg discs but is silenced in the wing disc, except when chromatin-mediated silencing is disrupted (Fig. S2A,B; Glicksman and Brower, 1988; Wang et al., 2010). *ubx* was not expressed in damaged wing discs, indicating that tissue damage did not alleviate silencing at this locus (Fig. S2C-F). In addition, we examined overall levels of H3K4me3 and Histone 3 Lysine 27 (H3K27) trimethylation, which can indicate chromatin state. Changes in overall methylation levels can be detected in imaginal discs by immunostaining (Hallson et al., 2012). Immunostaining did not show overall increases or decreases in H3K4me3 or H3K27me3 in regenerating wing discs 24 h after tissue damage (recovery time 24 or R24; Fig. S2G-N). A previous report has noted increased H3K4me3 by immunostaining after induction of sporadic cell death in wing imaginal discs (Herrera and Morata, 2014) but did not specify when the increases were observed or whether they were observed in dying or surviving cells. Our results suggest that tissue damage did not induce global changes in levels of these histone methylation marks or the deregulation of an epigenetically controlled homeotic gene. Thus, Trx likely regulates chromatin at specific loci to regulate discrete processes that occur upon wing disc injury.

Analysis of the role of Trithorax during regeneration

To quantify gene expression during regeneration, we identified two genes, *gapdh2* (Tso et al., 1985) and *CG12703*, used as controls in previous studies of imaginal disc growth (Classen et al., 2009), that did not change relative expression after tissue damage (Fig. S3A). Using these reference controls and mRNA from whole wing imaginal discs, we detected elevated relative expression of genes that are upregulated after tissue damage, such as *puckered* and *cabut* (Blanco et al., 2010), or expressed only outside the ablation zone, such as *teashirt* (Wu and Cohen, 2002; Fig. S3B-D). Interestingly, *trx* itself was not upregulated in the damaged and regenerating wing discs (Fig. S3E).

Our analysis of Trx in regeneration has been carried out in trx^{E2}/+ tissue, because homozygous *trx* mutant animals are embryonic lethal (Kennison and Tamkun, 1988) and mitotic clones of *trx* homozygous tissue in imaginal discs fail to grow and are eliminated through programmed cell death (Kanda et al., 2013). The trx^{E2} allele has been used to assess the role of Trx in a variety of processes (Kanda et al., 2013; Klymenko and Müller, 2004; Maurange and Paro, 2002). Our genetic analysis, comparing this allele with a weaker *trx* allele (trx^{1}) and a chromosomal deficiency, suggests that it is a very strong hypomorph (Fig. S4). Thus, we sought to identify how regeneration was impaired in the trx^{E2}/+ mutant tissue.

Early regeneration is normal in trx^{E2}/+ tissue

We examined trx^{E2}/+ regenerating wing discs for a regeneration blastema, which is the zone of proliferating cells that forms by R24 (Kiehle and Schubiger, 1985; Smith-Bolton et al., 2009). The signaling molecule Wingless (Wg) is expressed in the regeneration blastema when damage is caused by a cut or by tissue ablation (Gibson and Schubiger, 1999; Schubiger et al., 2010; Smith-Bolton et al., 2009). Wg was expressed in the trx^{E2}/+ regenerating tissue (Fig. 2A-C). Furthermore, marking cells in S phase using EdU incorporation demonstrated that a blastema formed in the trx^{E2}/+ damaged wing discs (Fig. 2D-F). The intensity of 5-ethynyl-2′-deoxyuridine (EdU) immunostaining was not different between control and trx^{E2}/+ regenerating discs at R24 (Fig. 2G). We also used phospho-histone H3 to mark mitotic cells (Hendzel et al., 1997). At R24, we found no difference in the number of mitotic cells per area between control and trx^{E2}/+ regenerating discs (Fig. 2H-K). Although increases were detected in EdU incorporation in R48 trx^{E2}/+ regenerating discs both within and outside of the blastema, following a peak of *cyclinE* (*cycE*) expression (Richardson et al., 1993) at R24 (Fig. S5A-G), no increases were detected in the frequencies of cells in mitosis or in the expression of *cyclinA* (Lehner and O'Farrell, 1989) and *cyclinB* (Lehner and O'Farrell, 1990; Fig. S5H-M). Thus, the mutant tissue formed a blastema that appeared to proliferate appropriately.

To confirm that the wing primordium was regrowing at the same rate in control and trx^{E2}/+ regenerating discs, tissue size was compared by measuring the area of the wing disc that expressed the wing primordium marker *nubbin* (Ng et al., 1995). Average wing primordium size was not different between control and trx^{E2}/+ regenerating discs at R24 (Fig. 2L-N) or R48 (Fig. 2O-Q).

Trx is important for the developmental checkpoint that allows regeneration to occur

Given that the wing primordia in trx^{E2}/+ and control regenerating discs at R48 were the same size, the deficit in regeneration in the

Development (2015) 142, 3500-3511 doi:10.1242/dev.122564

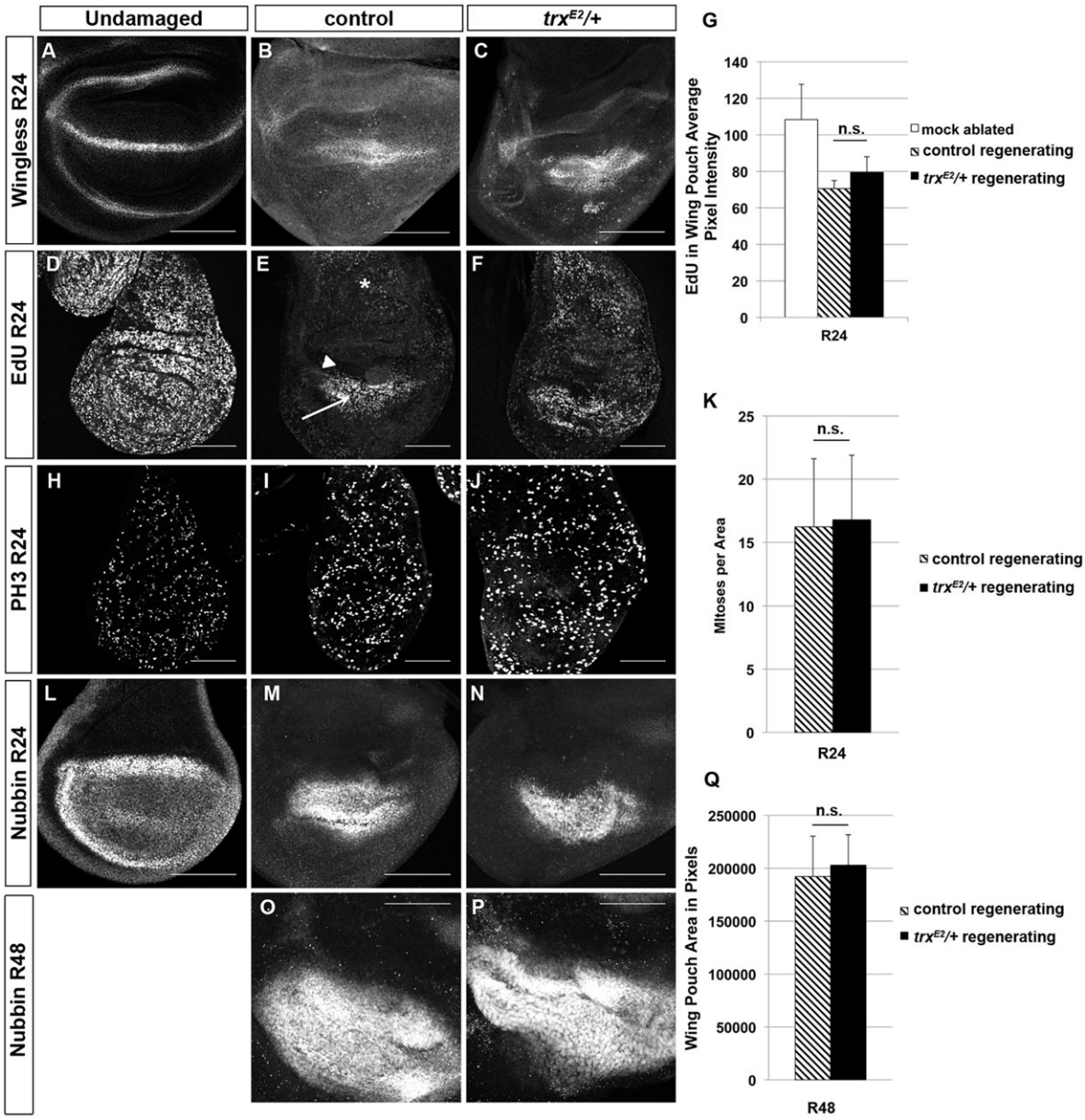

Fig. 2. Early regeneration is normal in *trx^{E2}*/+ mutant regenerating discs. (A-C) Anti-Wg in mock-ablated (A), control (B) and *trx^{E2}*/+ (C) regenerating wing discs at R24. (D-F) EdU incorporation marking cells in S phase in mock-ablated (D) as well as regenerating control (E) and *trx^{E2}*/+ (F) wing discs at R24. In E, arrow marks remaining wing pouch, arrowhead points to hinge region, and asterisk marks the notum. Similar results were obtained in three independent experiments. (G) Quantification of average pixel intensity of EdU staining in the wing pouch, identified by morphological features and Nubbin immunostaining, at R24. *n* was between six and 23 discs per genotype from two independent replicates, *P*=0.36. (H-J) PH3 immunostaining in mitotic cells in mock-ablated (H), regenerating control (I) and *trx^{E2}*/+ (J) imaginal wing discs at R24. Similar results were obtained in three independent experiments. (K) Quantification of mitotic cells per area in the wing pouch at R24. *n* was between 12 and 16 discs per genotype from two independent experiments, *P*=0.81. (L-P) Nubbin immunostaining marking the wing pouch in undamaged (L), regenerating control (M) and *trx^{E2}*/+ (N) discs at R24, and regenerating control (O) and *trx^{E2}*/+ (P) discs at R48. Undamaged R48 equivalent discs have pupariated and everted. (Q) Quantification of wing pouch area as measured by number of pixels in Nubbin-stained area at R48. *n*=12-16 discs per genotype, *P*=0.4. Similar results were obtained in two independent experiments. Error bars in G show s.e.m. Error bars in K and Q show s.d. n.s., not significant. R, number of hours after tissue damage. Scale bars: 100 µm.

trx^{E2}/+ tissue presumably occurred after this time. Immunostaining for cleaved Caspase 3 at R48 stained only pockets of debris, marked by absence of Nubbin and whole nuclei, and did not show any regenerated tissue undergoing apoptosis in *trx*/+ discs (Fig. 3A-H). Therefore, the *trx^{E2}*/+ regenerating tissue was not lost via apoptosis.

Tissue damage in imaginal discs activates a developmental checkpoint, which induces a delay in pupariation. This developmental delay requires retinoid synthesis and the insulin-like peptide dILP8 (Colombani et al., 2012; Garelli et al., 2012; Halme et al., 2010). To determine whether *trx^{E2}*/+ regenerating animals activated the developmental checkpoint, we quantified pupariation rates in undamaged and regenerating animals. Although normally developing *trx^{E2}*/+ and control animals pupariated at the same rate, *trx^{E2}*/+ animals with damaged wing discs appeared to pupariate approximately 1 day before control animals with damaged wing discs when new pupae were counted once a day (Fig. 3I). We confirmed this premature pupariation by quantifying the number of animals that had pupariated every 12 h (Fig. 3J). Therefore,

Development (2015) 142, 3500-3511 doi:10.1242/dev.122564

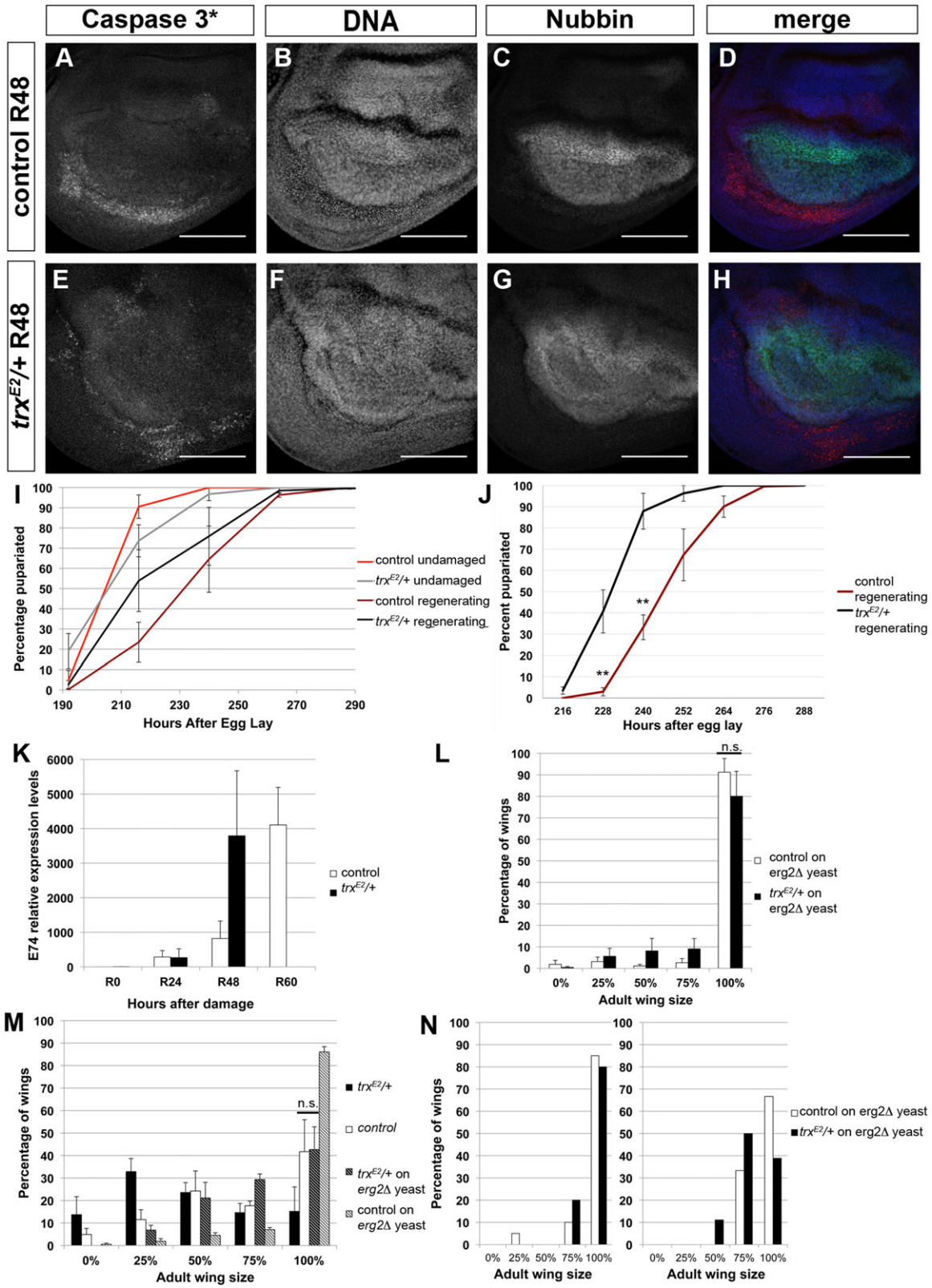

Fig. 3. See next page for legend.

although these two genotypes had regenerated to a similar extent at R48, the trx^{E2}/+ animals entered pupariation, while the control animals continued to regenerate for approximately 1 day more. Furthermore, use of RNAi to reduce Trx levels also led to premature pupariation (Fig. S6A,B).

These differences in timing of pupariation were due to differences in timing of Ecdysone signaling, as measured by expression of the Ecdysone-responsive gene *E74* (Fig. 3K; Burtis et al., 1990). Levels of *E74* expression remained low at R24 in control and trx^{E2}/+ larvae (Fig. 3K). However, *E74* expression had peaked at R48 in trx^{E2}/+

Development (2015) 142, 3500-3511 doi:10.1242/dev.122564

Fig. 3. *trx* heterozygous animals had reduced delay of pupariation. (A-H) Control (A-D) and trx^{E2}/+ (E-H) regenerating wing discs at R48. Cleaved Caspase 3 (A,E; red in merge), DNA (TO-PRO3; B,F; blue in merge), Nubbin (C,G; green in merge) and merge (D,H). The cleaved Caspase 3 observed was in the debris that remained adjacent to the healed and regenerating epithelium. (I) Pupariation rates (in hours after egg lay), with pupae counted every 24 h. Undamaged discs: three independent experiments, control n=100, trx^{E2}/+ n=62. Damaged discs: seven independent experiments, control n=362, trx^{E2}/+ n=225. (J) Pupariation rates (in hours after egg lay), with pupae counted every 12 h. Six independent experiments, control n=199, trx^{E2}/+ n=117. $^{**}P$<0.01 at 228 and 240 h. (K) Relative expression of *E74* quantified by qRT-PCR using whole larvae. Between three and six independent samples per time point. (L) Control and trx^{E2}/+ animals had adult wings of similar size after regeneration when grown on soft *erg2Δ* yeast food to delay pupariation. Eight independent experiments, control n=188 wings, trx^{E2}/+ n=92 wings. (M) trx^{E2}/+ regenerating animals grown on firm *erg2Δ* yeast food had adult wings similar in size to those of control regenerating animals grown on standard food. Control regenerating animals grown on *erg2Δ* yeast food delayed longer and had larger adult wings. Seven independent experiments, control animals fed standard food n=267 wings, trx^{E2}/+ animals fed standard food n=267 wings, control animals fed *erg2Δ* yeast food n=338 wings, trx^{E2}/+ animals fed *erg2Δ* yeast food n=144 wings. Percentages of animals with fully regenerated wings were not significantly different between control animals fed standard food and trx^{E2}/+ animals fed *erg2Δ* yeast food, P=0.96. (N) Two representative individual experiments in which animals grown on firm *erg2Δ* yeast food that pupariated in a 24 h window were collected and allowed to eclose. n was between 10 and 26 wings per genotype per 24 h window. All error bars are s.e.m. n.s., no significant difference in the frequency of fully regenerated wings. R, number of hours after tissue damage. Scale bars: 100 µm.

larvae, while *E74* expression in control larvae was only beginning to increase (Fig. 3K). Expression was high at R60 in control larvae, after all trx^{E2}/+ animals had pupariated (Fig. 3K).

We determined whether this early entry into pupariation halted regenerative proliferation by dissecting and staining regenerating wing discs at R56, when most trx^{E2}/+ animals had pupariated but control animals had not. The trx^{E2}/+ everted discs were significantly smaller than normal discs and folded abnormally, rendering them difficult to identify and image. However, PH3 immunostaining in the trx^{E2}/+ wing discs at R56 showed very few mitotic cells, demonstrating that regenerative proliferation had halted (Fig. S6C-E).

To determine whether this premature entry into pupariation accounted for the diminished regenerative capacity of the trx^{E2}/+ tissue, we artificially extended the third larval instar. Larvae fed on *erg2* mutant (*erg2Δ*) yeast fail to make Ecdysone, leading to a delay or absence of pupariation (Bos et al., 1976; Katsuyama and Paro, 2013; Parkin and Burnet, 1986). Transferring larvae to food made of *erg2Δ* yeast, agar and water 2 days after egg deposition delayed pupariation. The consistency of the *erg2Δ* yeast food affected the length of the pupariation delay. When transferred to softer *erg2Δ* yeast food, made with less agar, most larvae failed to pupariate. Those that did pupariate delayed by approximately 7 days (data not shown) and had fully regenerated wings (Fig. 3L). When transferred to firmer *erg2Δ* yeast food, made with more agar, larger numbers of larvae pupariated after a delay of 3-7 days. The trx^{E2}/+ animals grown on this firmer *erg2Δ* yeast food had wings comparable in size to those of control animals grown on standard food (Fig. 3M), showing rescue of the regeneration defect. However, control animals grown on the firmer *erg2Δ* yeast food delayed pupariation longer and had fully regenerated wings (Fig. 3M).

To compare control and trx^{E2}/+ regenerating animals with the same pupariation timing, we collected pupae that formed during 24 h windows and assessed their wings upon eclosion. Although variation occurred in individual experiments, trx^{E2}/+ animals had either similar or slightly reduced adult wing size compared with control animals (Fig. 3N). Thus, extending the time to pupariation largely rescued the regeneration defect of trx^{E2}/+ wing discs. Other, unidentified factors might account for the small remaining difference between trx^{E2}/+ and control regeneration.

dilp8 expression is reduced in *trx*/+ mutants

Given that dILP8 is expressed in damaged imaginal discs and is required for induction of the delay in pupariation (Colombani et al., 2012; Garelli et al., 2012), we examined *dilp8* expression. Interestingly, *dilp8* expression in trx^{E2}/+ regenerating discs was reduced at R24 compared with control regenerating discs (Fig. 4A).

The reduced *dilp8* expression could account for the shortened time for regeneration and smaller wings in trx^{E2}/+ animals. Indeed, animals heterozygous for the hypomorphic allele $dilp8^{MI00727}$ (Colombani et al., 2012) showed premature pupariation and reduced adult wings after damage (Fig. 4B,C). Importantly, overexpressing dILP8 using a *UAS-dilp8* transgene (Garelli et al., 2012) expressed via *rn-Gal4* during the thermal shift in the *rn*-expressing cells that survived ablation restored proper *dilp8* expression levels and rescued the premature pupariation phenotype in the trx^{E2}/+ regenerating animals, as well as overall wing size (Fig. 4D-F; Fig. S7A,B).

Because *dilp8* had significantly reduced expression in trx^{E2}/+ damaged tissue, it is possible that Trx is required to modify chromatin at the *dilp8* locus after wounding to alleviate silencing. However, the region around *dilp8* is characterized as open chromatin in S2 cells and lacks H3K4me3 and H3K27me3 in embryos, whole larvae and adults according to data deposited in the modENCODE database (Celniker et al., 2009; Kharchenko et al., 2011). Given that H3K4 becomes methylated at the start site of many transcriptionally active genes, including *dilp8* in regenerating tissue (data not shown), it is possible that Trx acts directly on the *dilp8* locus after tissue damage. However, it is also possible that Trx controls expression of a regulator of *dilp8*, either in the disc itself or in another tissue that impacts disc growth. Changing Ecdysone levels, by feeding the larvae either 20-hydroxyecdysone or *erg2Δ* yeast, did not affect *dilp8* expression (Fig. S7C,D). Therefore, we sought to identify a regulator of *dilp8* expression in the imaginal disc that is misregulated in the trx^{E2}/+ regenerating tissue.

JNK signaling is reduced in *trx*/+ mutants

Previous reports have suggested that JNK signaling regulates *dilp8* expression (Colombani et al., 2012; Katsuyama et al., 2015). Indeed, examination of the *dilp8* locus in GenomeSurveyor (Kazemian et al., 2011) shows conservation of a predicted AP-1 binding site (Perkins et al., 1988) about 4 kb upstream of the *dilp8* (CG14059) start site. If Trx acts through JNK signaling to regulate dILP8 expression, modification of JNK signaling might replicate or rescue the trx^{E2}/+ phenotype. Indeed, wing discs heterozygous mutant for the gene encoding JNK, *basket* (*bsk*) (Sluss et al., 1996), regenerated poorly as assessed by adult wing size, similar to wing discs heterozygous for trx^{E2} (Fig. 5A). In addition, increasing Puc levels via *rn-Gal4* and *UAS-puc* (Bischof et al., 2013) eliminated the normal damage-induced developmental delay and any regenerative response (Fig. 5B,C). Given the central role that JNK signaling plays in wound closure, regeneration and the damage-induced developmental delay, this complete abrogation of regeneration was not surprising.

To determine whether JNK signaling was reduced in trx^{E2}/+ regenerating wing discs, we assessed levels of phosphorylated JNK, expression of a transgenic reporter of JNK signaling (Chatterjee and Bohmann, 2012), and expression of the JNK signaling target gene *puckered* (*puc*) (Martín-Blanco et al., 1998). To assess levels of

Development (2015) 142, 3500-3511 doi:10.1242/dev.122564

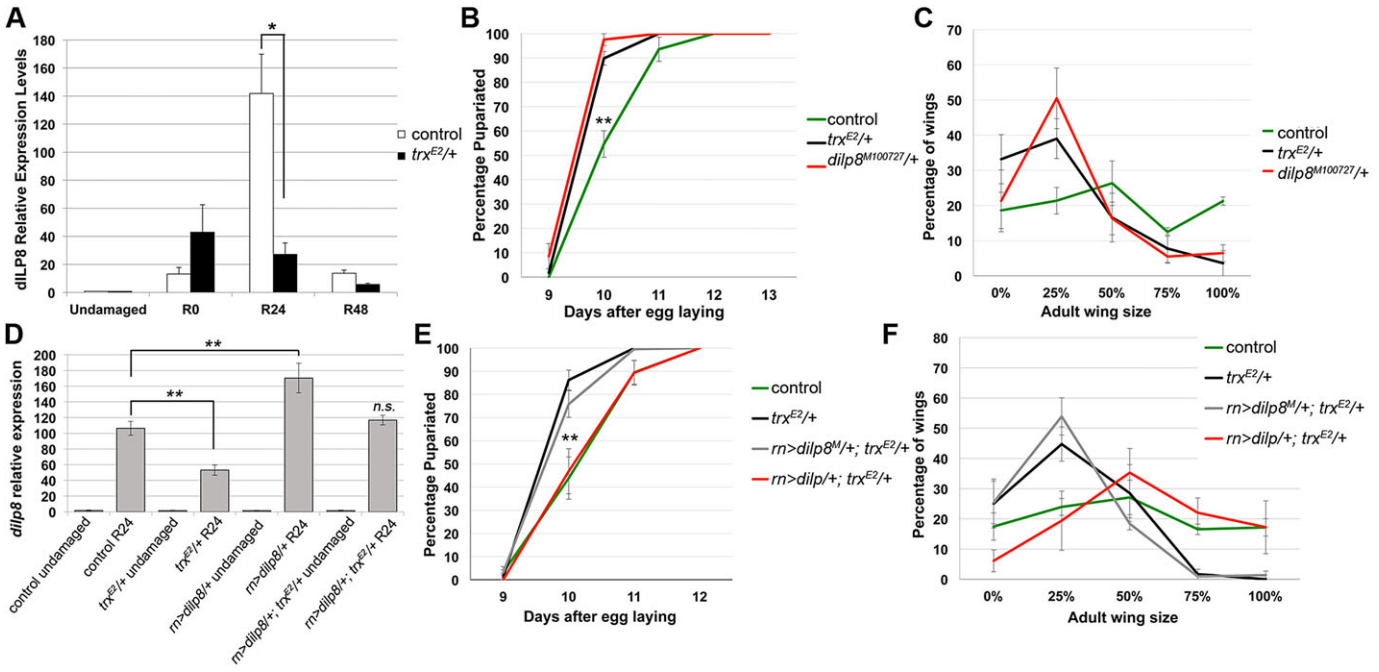

Fig. 4. Reduced expression of dILP8 accounts for premature pupariation in *trx*^{E2}/+ mutant regenerating animals. (A) Relative expression levels of *dilp8* quantified by qRT-PCR using undamaged discs and regenerating discs at R0, R24 and R48. Between two and five independent samples for each. *P<0.02. (B) Pupariation rates in control (n=97), *trx*^{E2}/+ (n=46) and *dilp8*^{MI00727}/+ (n=125) regenerating animals. Three independent experiments. At day 10, both *trx*^{E2}/+ and *dilp8*^{MI00727}/+ were significantly different from control, **P<0.01. *trx*^{E2}/+ and *dilp8*^{MI00727}/+ were not significantly different from each other. (C) Extent of regeneration as measured by adult wing size in control, *trx*^{E2}/+ and *dilp8*^{MI00727}/+ animals. Line graphs are used in this figure to make comparison of multiple genotypes easier. Three independent experiments, control n=170 wings, *trx*^{E2}/+ n=80 wings, *dilp8*^{MI00727}/+ n=196 wings. The distributions of wing sizes for *trx*^{E2}/+ and for *dilp8*^{MI00727}/+ were significantly different than for the control, χ^2 test P<0.01. (D) *dilp8* relative expression levels as measured by qRT-PCR in undamaged discs that remained at 18°C and thus lacked GAL4 activity as well as R24 regenerating discs in the noted genotypes. Note that at R24 *trx*^{E2}/+ caused a significant decrease in *dilp8* expression (**P<0.01), *rn>dilp8* led to significantly increased *dilp8* expression levels (**P<0.01), and rn>*dilp8* in the *trx*^{E2}/+ animals led to *dilp8* expression that was not significantly different from controls (n.s.). Three or four independent samples were used for each genotype and condition. (E) Pupariation rates in control (n=187), *trx*^{E2}/+ (n=78), *UAS-dilp8*^{M}/+; *trx*^{E2}/+ (n=157), and *UAS-dilp8/+; trx*^{E2}/+ (n=117) regenerating animals. *UAS-dilp8*^{M} expresses a mutant, inactive peptide. Six independent experiments. Differences between control and *UAS-dilp8/+; trx*^{E2}/+ and between *trx*^{E2}/+ and *UAS-dilp8*^{M}/+; *trx*^{E2}/+ at day 10 were not significant. Difference between *trx*^{E2}/+ and *UAS-dilp8/+; trx*^{E2}/+ at day 10 was significant, **P<0.01. (F) Extent of regeneration as measured by adult wing size in control (n=294 wings), *trx*^{E2}/+ (n=94 wings), *UAS-dilp8*^{M}/; *trx*^{E2}/+ (n=82 wings) and *UAS-dilp8/+; trx*^{E2}/+ (n=144 wings) regenerating animals. The distributions of adult wing sizes between *trx*^{E2}/+ and *UAS-dilp8/+; trx*^{E2}/+ were significantly different, χ^2 test P<0.01. Five independent experiments. All error bars are s.e.m. except in A and D, in which they are s.d. R, number of hours after tissue damage.

activated JNK, we immunostained regenerating discs using an anti-phospho-JNK antibody. In two independent experiments, phospho-JNK was significantly reduced in the *trx*^{E2}/+ regenerating discs (Fig. 5D-F).

To assess transcription downstream of JNK, we used a transgenic reporter (TRE-red) that consists of four AP-1 binding sites controlling expression of the *dsRED* gene (Chatterjee and Bohmann, 2012). This reporter measures activity of the JNK-dependent AP-1 transcriptional complex, which consists of Jun and Fos (Perkins et al., 1988). Expression of the TRE-red reporter mirrored that of the *puc-lacZ* enhancer trap after tissue damage in control imaginal discs (Fig. 5G-J). The dsRed was observed in the regenerating tissue, as well as in the cellular debris that remained adjacent to the epithelium and was occasionally present in the images. To quantify levels of dsRed in the blastema, we calculated the average pixel intensity in the blastema, which was defined by Wg expression. Levels of dsRed remained elevated throughout regeneration, owing to either continued signaling or dsRed perdurance (Fig. 5K).

To compare transcription downstream of JNK signaling in control and *trx*^{E2}/+ wounded discs, we imaged and quantified dsRed in the blastema at R24 (Fig. 5L-U). In two independent experiments, dsRed expression was significantly reduced in the *trx*^{E2}/+ regenerating tissue compared with control regenerating tissue at R24 (Fig. 5U). In a third experiment, expression was highly variable and not statistically different between the genotypes (data not shown). Given that *dilp8* expression, phospho-JNK levels and the TRE-red reporter were all reduced in the mutant regeneration blastema, we concluded that JNK signaling was reduced.

Misregulation of *puc* represses JNK signaling in *trx*/+ mutant regenerating tissue

As a third assessment of transcription downstream of JNK signaling, we assessed expression of the target gene *puc*, which encodes a phosphatase that dephosphorylates and negatively regulates JNK (Martín-Blanco et al., 1998). To our surprise, *puc* expression levels were significantly elevated in the *trx*^{E2}/+ regenerating tissue compared with control regenerating tissue at R24, as measured by both an enhancer trap (Ring and Martinez Arias, 1993) and qRT-PCR of *puc* mRNA (Fig. 6A-C). This result raised the possibility that Trx negatively regulates *puc* and that the elevated *puc* caused the reduction of JNK signaling and *dilp8* expression in the *trx*^{E2}/+ mutant (Fig. 6D). Importantly, RNAi against *trx* also caused an increase in *puc* expression and a reduction in *dilp8* expression (Fig. S8).

To confirm that elevated *puc* expression was responsible for the decrease in *dilp8* expression, we quantified *dilp8* expression in regenerating discs that were heterozygous mutant for both *trx* and *puc*. In these doubly heterozygous mutant animals, *puc* expression

Development (2015) 142, 3500-3511 doi:10.1242/dev.122564

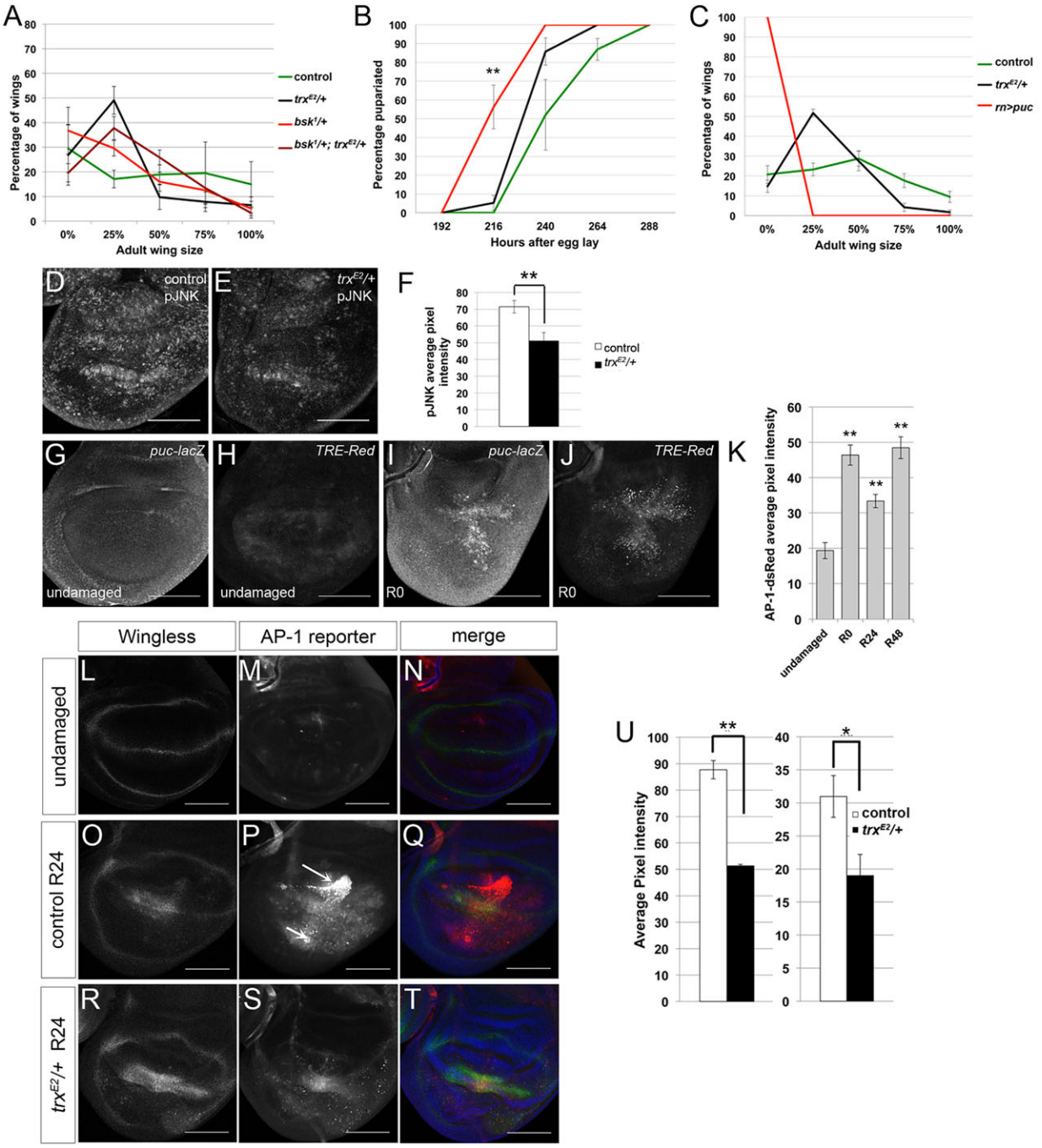

Fig. 5. JNK signaling is reduced in *trx^{E2}*/+ mutant regenerating tissue. (A) Extent of regeneration as measured by adult wing size. Note that the *trx^{E2}*/+, *bsk^{1}*/+ and *bsk^{1}*/+; *trx^{E2}*/+ animals all consistently regenerated poorly relative to control animals, although the differences among the mutants were not statistically significant at each wing size and were highly variable across experiments, possibly owing in part to high lethality in the *bsk^{1}*/+ and *bsk^{1}*/+; *trx^{E2}*/+ regenerating animals. Three independent experiments, control n=70 wings, *trx^{E2}*/+ n=54 wings, *bsk^{1}*/+ n=122 wings, *bsk^{1}*/+; *trx^{E2}*/+ n=162 wings. (B) Pupariation timing of regenerating animals (in hours after egg lay). *UAS-puc* was expressed under the control of *rn-GAL4*. The difference in pupariation at 216 h between control and *rn>puc* was significant, $^{**}P$<0.01. Three independent experiments, control n=158 pupae, *trx^{E2}*/+ n=117 pupae, *rn>puc* n=64 pupae. (C) Extent of regeneration as measured by adult wing size. The distributions of adult wing sizes between control and *rn>puc* were significantly different, χ^2 test P<0.01. Four independent experiments, control n=325 wings, *trx^{E2}*/+ n=270 wings, *rn>puc* n=114 wings. (D,E) Phosph-JNK immunostaining in control (D) and *trx^{E2}*/+ (E) R24 discs. (F) Quantification of phospho-JNK staining in the blastema as defined by Nubbin expression. Control and *trx^{E2}*/+ n=9 discs each. $^{**}P$<0.01. (G-J) Expression of the *puc-lacZ* (G,I) and *TRE-Red* (H,J) reporters in undamaged (G,H) and damaged (I,J) wing discs. (K) Quantification of dsRed average pixel intensity in the wing pouch or regeneration blastema in undamaged wing discs (n=4), as well as regenerating discs at R0 (n=14), R24 (n=6) and R48 (n=7). $^{**}P$<0.01 compared with undamaged discs. (L-T) Wing imaginal discs showing anti-Wg (L,O,R), dsRED (M,P,S) and the merge of Wg (green), dsRED (red) and DAPI (blue) (N,Q,T). Images are of a mock-ablated wing disc (L-N), a control disc at R24 (O-Q) and a *trx^{E2}*/+ disc at R24 (R-T). Arrows mark cellular debris, which was retained in disc folds at similar frequencies in all ablated genotypes. (U) Quantification of AP-1 reporter expression in the Wg-expressing blastema in two independent experiments. Pockets of debris occurred randomly in all genotypes and were excluded from the analysis. Examples are marked by arrows in P and confirmed by absence of nuclear DAPI staining. $^{**}P$=3×10^{-5}. Control n=7 discs. *trx^{E2}*/+ n=4 discs. $^{*}P$=0.02. Control n=10 discs, *trx^{E2}*/+ n=11 discs. Scale bars: 100 µm. All error bars are s.e.m. R, number of hours after tissue damage.

Development (2015) 142, 3500-3511 doi:10.1242/dev.122564

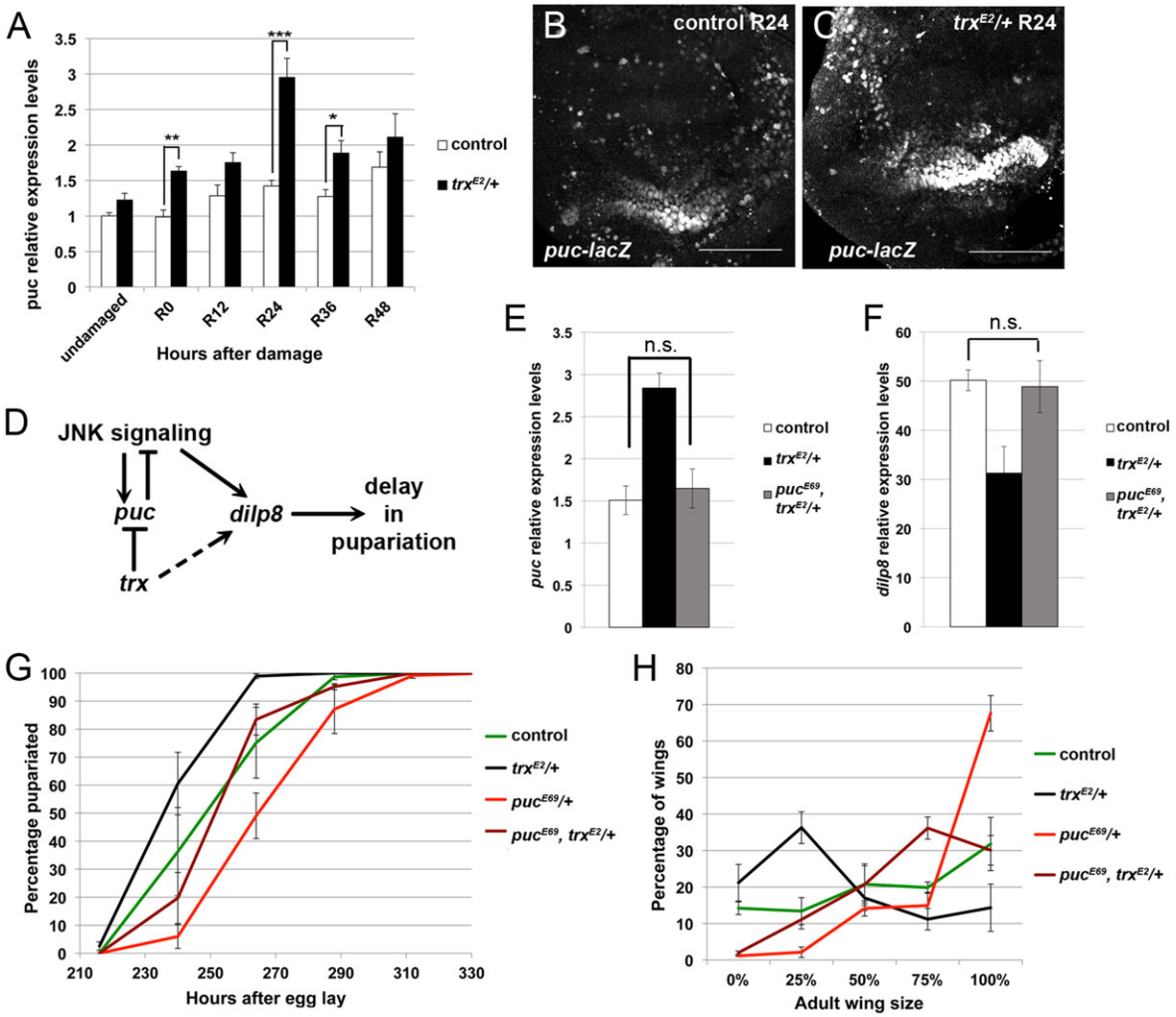

Fig. 6. Increased *puc* expression limits *dilp8* expression and regenerative capacity. (A) Relative expression levels of *puc* quantified by qRT-PCR in undamaged and regenerating wing discs. *n* was between five and ten independent samples per genotype and time point. **P*<0.02, ***P*<0.0005, ****P*<5×10^{-5}. (B,C) Anti-β-galactosidase immunostaining of discs containing the *puc-lacZ* enhancer trap. Scale bars: 100 µm. (B) Control disc at R24. (C) *trx*^{E2}/+ disc at R24. Similar results were obtained in three independent experiments. (D) Model showing *trx* negatively regulating *puc* expression, which regulates JNK signaling and *dilp8* expression. Regulation of *dilp8* by *trx* independently of JNK is also possible. Arrows do not imply direct interaction. (E) Relative expression levels of *puc*, determined by qRT-PCR, in regenerating wing discs. *P*=0.66, indicating no significant difference (n.s.). control *n*=4, *trx*^{E2}/+ *n*=5, *puc*^{e69}, *trx*^{E2}/+ *n*=5 independent biological replicates. (F) Relative expression levels of *dilp8* determined by qRT-PCR, in regenerating wings discs. *P*=0.82, indicating no significant difference (n.s.). control *n*=5, *trx*^{E2}/+ *n*=4, *puc*^{e69}, *trx*^{E2}/+ *n*=5 independent biological replicates. (G) Pupariation timing of regenerating animals (in hours after egg lay). The differences between control and *puc*^{e69}, *trx*^{E2}/+ were not significant. Four independent experiments. Control *n*=97, *puc*^{E69}/+ *n*=80, *trx*^{E2}/+ *n*=36, *puc*^{E69}, *trx*^{E2}/+ *n*=128. (H) Extent of regeneration as measured by adult wing size. All results are significantly different from each other, χ^2 *P*<0.01. Four independent experiments, control *n*=263 wings, *puc*^{E69}/+ *n*=246 wings, *trx*^{E2}/+ *n*=130 wings, *puc*^{E69}, *trx*^{E2}/+ *n*=377 wings. Scale bars: 100 µm. All error bars are s.e.m. R, number of hours after tissue damage.

was similar to expression in control regenerating tissue (Fig. 6E). Importantly, *dilp8* expression levels were similar to expression levels in control regenerating discs (Fig. 6F). These animals pupariated at the same time as control regenerating animals and regenerated to the same extent as control animals (Fig. 6G,H). Thus, reduction of *puc* in the *trx*^{E2}/+ regenerating tissue restored systemic signaling, developmental timing and regenerative capacity. Although the genetic interaction experiments alone can only suggest a regulatory relationship, the changes in *puc* expression, phospho-JNK levels and the *AP1-dsRED* reporter in the *trx*^{E2}/+ regenerating tissue, as well as the restoration of proper *puc* and *dilp8* expression levels in the *puc*^{E69}, *trx*^{E2}/+ regenerating tissue, indicate that *puc* expression and JNK activity are downstream of *trx*. As Trx is generally thought to promote rather than repress gene expression, Trx is not likely to act directly on the *puc* locus in the damaged tissue. Therefore, we propose that Trx regulates expression of an unknown factor, which in turn regulates *puc* expression.

DISCUSSION

This work sought to identify the role that the chromatin modifier Trx plays in regulating regeneration. Our results demonstrate that the primary problem in *trx* heterozygous regenerating animals was insufficient time for regeneration. We propose a model in which reduced Trx levels lead to abnormally high expression of *puc*, which suppresses JNK signaling, which leads to insufficient *dilp8* expression (Bosch et al., 2008, 2005; Colombani et al., 2012). Although JNK signaling was reduced in the *trx* heterozygous tissue, it was still sufficient to promote wound healing, blastema formation

Development (2015) 142, 3500-3511 doi:10.1242/dev.122564

and regenerative growth. Thus, *dilp8* expression seems more sensitive to changes in JNK signaling than other transcriptional targets of this pathway or it might require additional input from a Trx-dependent but JNK-independent mechanism (Fig. 6D). It is likely that further reduction in Trx levels or activity would impair other JNK-dependent aspects of regeneration. Thus, we have identified a Trx-dependent mechanism that controls the scope and magnitude of regeneration signaling.

It is possible that Trx regulates JNK signaling in a similar manner in other contexts. Indeed, *puc* expression levels appeared to be slightly increased in undamaged trx^{E2}/+ discs compared with controls (Fig. 6A), and phospho-JNK levels appeared to be reduced outside the regeneration blastema in trx^{E2}/+ discs (Fig. 5D,E). Interestingly, when a *trx* RNAi construct was expressed in the developing notum, adult flies had a weak notum malformation phenotype, while a *bsk* RNAi construct induced a moderate notum malformation phenotype, suggesting that Trx can affect the JNK-dependent process of notum fusion (Mummery-Widmer et al., 2009). Furthermore, animals homozygous for one mutant allele, trx^{00347}, are reported to have a groove in the adult notum suggestive of incomplete notum fusion ('Insertion alleles', communication to Flybase by Berkeley Drosophila Genome Project, 1993). To our knowledge, however, no report has implicated Trx in regulation of the JNK-dependent process of embryonic dorsal closure or described a dorsal closure phenotype for any *trx* allele.

We do not yet know how Trx regulates *puc* expression after tissue damage. The *puc* region contains histone modifications and binds chromatin modifiers, including members of the NURF complex and Polycomb, according to the modENCODE database (Celniker et al., 2009). Although these modENCODE data are not from isolated imaginal discs, these findings suggest that regulatory mechanisms other than AP-1 are likely to contribute to the control of *puc* expression throughout development. Our results caution against using *puc* expression as the sole indicator of JNK signaling activity. As Trx is generally thought to promote rather than repress gene expression, Trx might regulate a repressor of *puc* expression. Indeed, GenomeSurveyor (Kazemian et al., 2011) predicts binding sites for many transcription factors in the *cis*-regulatory modules defined by the AP-1 binding sites in the *puc* locus. Several of these predicted binding factors can act as repressors of transcription and are in turn located in genomic regions that, according to modENCODE data, contain highly modified chromatin, and thus are candidates for mediating the influence of Trx on *puc*. We tested mutants of the five genes that we identified as fitting these criteria: *sloppy-paired 1*, *tramtrack*, *caupolican*, *traffic jam* and *earmuff* (Gómez-Skarmeta et al., 1996; Grossniklaus et al., 1992; Harrison and Travers, 1990; Kawashima et al., 2003; Weng et al., 2010). None of the mutants had impaired regeneration; therefore, none is likely to be the factor that regulates *puc* downstream of *trx* (Fig. S9A-E), which remains to be identified.

We had initially predicted broad changes in gene expression in the *trx* mutant regenerating tissue, resulting in multiple defects throughout the regeneration process. However, expression of many of the regeneration genes we tested was not impaired (Fig. S9F,G), possibly because the *trx* heterozygote reduces the gene dosage only by half. Strong changes in expression were detected in only a few specific genes, such as *cycE*, *puc* and *dilp8*. However, it remains possible and even likely that additional genes are regulated by Trx after tissue damage that were not detectable in the heterozygous mutant. Indeed, chromatin modification could rapidly and efficiently alter the developmental program in damaged tissue to enable regeneration. Importantly, RNAi knockdown of the planarian homolog of *trx*, *Smed-mll1/2*, did not prevent formation of a regeneration blastema but did impair regeneration of particular cells (Hubert et al., 2014), suggesting that Trx and its homologs play specific roles in regeneration across species.

In summary, our unbiased genetic screen identified a chromatin-modification gene, *trx*, as a key regulator of regeneration. Reducing levels of Trx in damaged tissue led to reduced JNK signaling and limited dILP8 expression, resulting in a failure to complete regenerative growth before the onset of pupariation and metamorphosis. Thus, we have proposed a model in which Trx is important for regulating the expression of the phosphatase Puckered, which modulates JNK activity. We have not ruled out the possibility that Trx also regulates *dilp8* directly or that it regulates additional regulators of *dilp8* expression. This work has demonstrated that chromatin modification after wounding can regulate specific signaling events and expression of key genes. A genome-wide examination of changes in histone modification and chromatin state in regenerating tissue will identify more genes that are regulated epigenetically upon wounding, including novel regeneration genes that will contribute to our understanding of wound repair. Our findings also illustrate the importance of fine-tuned regulation of regeneration signaling, because changes in the magnitude or duration of feedback inhibition can significantly alter the regenerative outcome.

MATERIALS AND METHODS

Tissue ablation and genetic screen

Ablation was induced as previously described (Smith-Bolton et al., 2009), using expression of *UAS-reaper* and a 24 h thermal shift to 30°C to induce cell death. The genetic screen was carried out as previously described (Smith-Bolton et al., 2009). For all experiments, ablation was induced in the early third instar, which is 7 days after egg laying at 18°C. Mock-ablated controls experienced the shift to 30°C for 24 h alongside the ablating animals, but lacked the ablation-inducing transgenes.

Fly lines and genetics

Flies were maintained on standard molasses-based food. Regeneration experiments were carried out on modified Bloomington standard media containing malt and 0.3% tegosept (Apex). Fly lines were obtained from the Bloomington *Drosophila* Stock Center, FlyORF, the Vienna *Drosophila* Resource Center or colleagues (see supplementary materials and methods for details).

Imaging adult wings

Adult wings were mounted in Gary's Magic Mount [Canada balsam (Sigma) dissolved in methyl salicylate (Sigma)]. Images were taken on an Olympus SZX10 microscope using CellSens Dimension software with the Extended Focal Image feature. Wing area was measured in ImageJ. Samples included both females and males. Undamaged control wings were averaged to give a standard area. The area of each experimental wing was then calculated as a fraction of the standard. Trichomes were counted in ImageJ within a 50×50 pixel box.

Immunohistochemistry

Immunostaining was carried out as previously described (Smith-Bolton et al., 2009). Wing discs were imaged on a Zeiss LSM 510 or a Zeiss LSM 700 confocal microscope. Images were processed using ZEN lite (Zeiss), ImageJ (NIH) and Photoshop (Adobe). Details for antibodies, labeling and image analysis can be found in supplementary materials and methods.

Molecular biology

qRT-PCR was carried out as previously described (Classen et al., 2009). Wing disc tissue was used for all experiments except the *E74* qRT-PCR, in which whole larvae were used. For qRT-PCR of whole larvae, mRNA was

Development (2015) 142, 3500-3511 doi:10.1242/dev.122564

extracted using the Omega Total RNA Kit II (VWR). Independent samples consisted of 15 wing discs or five whole larvae. Power SYBR Green Master Mix (ABI) was used and reactions were run on an ABI Step One Plus Real-Time PCR System. Analysis was done by the $\Delta\Delta C_T$ method and expression levels were normalized to *gapdh2*. Fold changes relative to control undamaged discs are shown. For all primer sequences, sources for primer sequences or sources for primers, see Table S1. The variation observed in fold changes for *dilp8* at R24 was probably because expression levels in undamaged discs were extremely low.

Pupariation quantification and Ecdysone manipulation

Pupariation rates were quantified by counting newly formed pupae every 12 or 24 h. Pupariation was delayed by raising larvae on food made of *erg2Δ* mutant yeast, strain 4020788 (ATCC, Manassas, VA, USA). Food was prepared as previously described (Katsuyama and Paro, 2011). Soft food contained 6.5% agar. Firm food contained 7.5% agar. Eggs were laid on grape plates, from which larvae were picked on day 2 after egg laying, and transferred to *erg2Δ* yeast food, 50 larvae per vial. To compare regeneration in animals that pupariated at the same time, pupae formed within 24 h windows were transferred to fresh vials. 20-Hydroxyecdysone (Sigma) was fed to the larvae at a concentration of 0.6 mg/ml of food in a microfuge tube as previously described (Halme et al., 2010). Controls that were not fed 20-hydroxyecdysone were in tubes that contained vehicle (ethanol) only mixed with the food.

Statistical analysis

All statistical analyses were performed using Student's *t*-test in Excel except where noted that χ^2 tests were used. Results were considered statistically significant with $P<0.02$.

Acknowledgements

The authors would like to thank A. Brock and P. Newmark for critical reading of the manuscript and helpful discussions; D. Bohmann, M. Dominguez and S. Cohen for reagents; the Bloomington *Drosophila* Stock Center (NIH P40OD018537); the TRiP at Harvard Medical School (NIH/NIGMS R01-GM084947); the VDRC; and the Developmental Studies Hybridoma Bank (NICHD, University of Iowa).

Competing interests

The authors declare no competing or financial interests.

Author contributions

R.K.S.-B. and A.S. designed the approach, R.K.S.-B., A.S. and S.J.K. designed, carried out and interpreted the experiments, and R.K.S.-B. prepared the manuscript.

Funding

This work was funded by a Young Investigator Award from The Roy J. Carver Charitable Trust [#12-4041].

Supplementary information

Supplementary information available online at
http://dev.biologists.org/lookup/suppl/doi:10.1242/dev.122564/-/DC1

References

Ardehali, M. B., Mei, A., Zobeck, K. L., Caron, M., Lis, J. T. and Kusch, T. (2011). Drosophila Set1 is the major histone H3 lysine 4 trimethyltransferase with role in transcription. *EMBO J.* **30**, 2817-2828.

Bergantiños, C., Corominas, M. and Serras, F. (2010). Cell death-induced regeneration in wing imaginal discs requires JNK signalling. *Development* **137**, 1169-1179.

Bischof, J., Björklund, M., Furger, E., Schertel, C., Taipale, J. and Basler, K. (2013). A versatile platform for creating a comprehensive UAS-ORFeome library in Drosophila. *Development* **140**, 2434-2442.

Blanco, E., Ruiz-Romero, M., Beltran, S., Bosch, M., Punset, A., Serras, F. and Corominas, M. (2010). Gene expression following induction of regeneration in Drosophila wing imaginal discs. Expression profile of regenerating wing discs. *BMC Dev. Biol.* **10**, 94.

Bos, M., Burnet, B., Farrow, R. and Woods, R. A. (1976). Development of Drosophila on sterol mutants of the yeast Saccharomyces cerevisiae. *Genet. Res.* **28**, 163-176.

Bosch, M., Serras, F., Martín-Blanco, E. and Baguñà, J. (2005). JNK signaling pathway required for wound healing in regenerating Drosophila wing imaginal discs. *Dev. Biol.* **280**, 73-86.

Bosch, M., Baguñ, J. and Serras, F. (2008). Origin and proliferation of blastema cells during regeneration of Drosophila wing imaginal discs. *Int. J. Dev. Biol.* **52**, 1043-1050.

Breen, T. R. (1999). Mutant alleles of the Drosophila trithorax gene produce common and unusual homeotic and other developmental phenotypes. *Genetics* **152**, 319-344.

Breen, T. R. and Harte, P. J. (1991). Molecular characterization of the trithorax gene, a positive regulator of homeotic gene expression in Drosophila. *Mech. Dev.* **35**, 113-127.

Brook, W. J. and Cohen, S. M. (1996). Antagonistic interactions between wingless and decapentaplegic responsible for dorsal-ventral pattern in the Drosophila Leg. *Science* **273**, 1373-1377.

Burtis, K. C., Thummel, C. S., Jones, C. W., Karim, F. D. and Hogness, D. S. (1990). The Drosophila 74EF early puff contains E74, a complex ecdysone-inducible gene that encodes two ets-related proteins. *Cell* **61**, 85-99.

Celniker, S. E., Dillon, L. A. L., Gerstein, M. B., Gunsalus, K. C., Henikoff, S., Karpen, G. H., Kellis, M., Lai, E. C., Lieb, J. D., MacAlpine, D. M. et al. (2009). Unlocking the secrets of the genome. *Nature* **459**, 927-930.

Chatterjee, N. and Bohmann, D. (2012). A versatile ΦC31 based reporter system for measuring AP-1 and Nrf2 signaling in Drosophila and in tissue culture. *PLoS ONE* **7**, e34063.

Classen, A.-K., Bunker, B. D., Harvey, K. F., Vaccari, T. and Bilder, D. (2009). A tumor suppressor activity of Drosophila Polycomb genes mediated by JAK-STAT signaling. *Nat. Genet.* **41**, 1150-1155.

Colombani, J., Andersen, D. S. and Léopold, P. (2012). Secreted peptide Dilp8 coordinates Drosophila tissue growth with developmental timing. *Science* **336**, 582-585.

Dietzl, G., Chen, D., Schnorrer, F., Su, K.-C., Barinova, Y., Fellner, M., Gasser, B., Kinsey, K., Oppel, S., Scheiblauer, S. et al. (2007). A genome-wide transgenic RNAi library for conditional gene inactivation in Drosophila. *Nature* **448**, 151-156.

Elliott, S. A. and Sánchez Alvarado, A. (2013). The history and enduring contributions of planarians to the study of animal regeneration. *Wiley Interdiscip. Rev. Dev. Biol.* **2**, 301-326.

Fukuda, A., Morris, J. P. and Hebrok, M. (2012). Bmi1 is required for regeneration of the exocrine pancreas in mice. *Gastroenterology* **143**, 821-831.e1-2.

Galliot, B. (2012). Hydra, a fruitful model system for 270 years. *Int. J. Dev. Biol.* **56**, 411-423.

Garelli, A., Gontijo, A. M., Miguela, V., Caparros, E. and Dominguez, M. (2012). Imaginal discs secrete insulin-like peptide 8 to mediate plasticity of growth and maturation. *Science* **336**, 579-582.

Gemberling, M., Bailey, T. J., Hyde, D. R. and Poss, K. D. (2013). The zebrafish as a model for complex tissue regeneration. *Trends Genet.* **29**, 611-620.

Gibson, M. C. and Schubiger, G. (1999). Hedgehog is required for activation of engrailed during regeneration of fragmented Drosophila imaginal discs. *Development* **126**, 1591-1599.

Glicksman, M. A. and Brower, D. L. (1988). Misregulation of homeotic gene expression in Drosophila larvae resulting from mutations at the extra sex combs locus. *Dev. Biol.* **126**, 219-227.

Gómez-Skarmeta, J.-L., del Corral, R. D., de la Calle-Mustienes, E., Ferré-Marcó, D. and Modolell, J. (1996). Araucan and caupolican, two members of the novel iroquois complex, encode homeoproteins that control proneural and vein-forming genes. *Cell* **85**, 95-105.

Gouge, C. A. and Christensen, T. W. (2010). Detection of S Phase in multiple Drosophila tissues utilizing the EdU labeling technique. *Dros. Inf. Serv.* **93**, 203-212.

Grimaud, C., Negre, N. and Cavalli, G. (2006). From genetics to epigenetics: the tale of Polycomb group and trithorax group genes. *Chromosome Res.* **14**, 363-375.

Grossniklaus, U., Pearson, R. K. and Gehring, W. J. (1992). The Drosophila sloppy paired locus encodes two proteins involved in segmentation that show homology to mammalian transcription factors. *Genes Dev.* **6**, 1030-1051.

Hallson, G., Hollebakken, R. E., Li, T., Syrzycka, M., Kim, I., Cotsworth, S., Fitzpatrick, K. A., Sinclair, D. A. R. and Honda, B. M. (2012). dSet1 is the main H3K4 di- and tri-methyltransferase throughout Drosophila development. *Genetics* **190**, 91-100.

Halme, A., Cheng, M. and Hariharan, I. K. (2010). Retinoids regulate a developmental checkpoint for tissue regeneration in Drosophila. *Curr. Biol.* **20**, 458-463.

Harrison, S. D. and Travers, A. A. (1990). The tramtrack gene encodes a Drosophila finger protein that interacts with the ftz transcriptional regulatory region and shows a novel embryonic expression pattern. *EMBO J.* **9**, 207-216.

Hazelrigg, T., Levis, R. and Rubin, G. M. (1984). Transformation of white locus DNA in drosophila: dosage compensation, zeste interaction, and position effects. *Cell* **36**, 469-481.

Hendzel, M. J., Wei, Y., Mancini, M. A., Van Hooser, A., Ranalli, T., Brinkley, B. R., Bazett-Jones, D. P. and Allis, C. D. (1997). Mitosis-specific phosphorylation of histone H3 initiates primarily within pericentromeric heterochromatin during G2 and spreads in an ordered fashion coincident with mitotic chromosome condensation. *Chromosoma* **106**, 348-360.

Herrera, S. C. and Morata, G. (2014). Transgressions of compartment boundaries and cell reprogramming during regeneration in Drosophila. *Elife* **3**, e01831.
Hubert, A., Henderson, J. M., Ross, K. G., Cowles, M. W., Torres, J. and Zayas, R. M. (2014). Epigenetic regulation of planarian stem cells by the SET1/MLL family of histone methyltransferases. *Epigenetics* **8**, 79-91.
Ingham, P. and Whittle, R. (1980). Trithorax: a new homoeotic mutation of Drosophila melanogaster causing transformations of abdominal and thoracic imaginal segments. *Mol. Gen. Genet.* **179**, 607-614.
Jin, Y., Xu, J., Yin, M.-X., Lu, Y., Hu, L., Li, P., Zhang, P., Yuan, Z., Ho, M. S., Ji, H. et al. (2013). Brahma is essential for Drosophila intestinal stem cell proliferation and regulated by Hippo signaling. *Elife* **2**, e00999.
Kanda, H., Nguyen, A., Chen, L., Okano, H. and Hariharan, I. K. (2013). The Drosophila ortholog of MLL3 and MLL4, trithorax related, functions as a negative regulator of tissue growth. *Mol. Cell. Biol.* **33**, 1702-1710.
Katsuyama, T. and Paro, R. (2011). Epigenetic reprogramming during tissue regeneration. *FEBS Lett.* **585**, 1617-1624.
Katsuyama, T. and Paro, R. (2013). Innate immune cells are dispensable for regenerative growth of imaginal discs. *Mech. Dev.* **130**, 112-121.
Katsuyama, T., Comoglio, F., Seimiya, M., Cabuy, E. and Paro, R. (2015). During Drosophila disc regeneration, JAK/STAT coordinates cell proliferation with Dilp8-mediated developmental delay. *Proc. Natl. Acad. Sci. USA* **112**, E2327-E2336.
Kawashima, T., Nakamura, A., Yasuda, K. and Kageyama, Y. (2003). Dmaf, a novel member of Maf transcription factor family is expressed in somatic gonadal cells during embryonic development and gametogenesis in Drosophila. *Gene Expr. Patterns* **3**, 663-667.
Kazemian, M., Brodsky, M. H. and Sinha, S. (2011). Genome Surveyor 2.0: cis-regulatory analysis in Drosophila. *Nucleic Acids Res.* **39**, W79-W85.
Kennison, J. A. and Tamkun, J. W. (1988). Dosage-dependent modifiers of polycomb and antennapedia mutations in Drosophila. *Proc. Natl. Acad. Sci. USA* **85**, 8136-8140.
Kharchenko, P. V., Alekseyenko, A. A., Schwartz, Y. B., Minoda, A., Riddle, N. C., Ernst, J., Sabo, P. J., Larschan, E., Gorchakov, A. A., Gu, T. et al. (2011). Comprehensive analysis of the chromatin landscape in Drosophila melanogaster. *Nature* **471**, 480-485.
Kiehle, C. P. and Schubiger, G. (1985). Cell proliferation changes during pattern regulation in imaginal leg discs of Drosophila melanogaster. *Dev. Biol.* **109**, 336-346.
Klymenko, T. and Müller, J. (2004). The histone methyltransferases Trithorax and Ash1 prevent transcriptional silencing by Polycomb group proteins. *EMBO Rep.* **5**, 373-377.
Kuzin, B., Tillib, S., Sedkov, Y., Mizrokhi, L. and Mazo, A. (1994). The Drosophila trithorax gene encodes a chromosomal protein and directly regulates the region-specific homeotic gene fork head. *Genes Dev.* **8**, 2478-2490.
Lai, Z. C. and Li, Y. (1999). Tramtrack69 is positively and autonomously required for Drosophila photoreceptor development. *Genetics* **152**, 299-305.
Lee, N., Maurange, C., Ringrose, L. and Paro, R. (2005). Suppression of Polycomb group proteins by JNK signalling induces transdetermination in Drosophila imaginal discs. *Nature* **438**, 234-237.
Lehner, C. F. and O'Farrell, P. H. (1989). Expression and function of Drosophila cyclin A during embryonic cell cycle progression. *Cell* **56**, 957-968.
Lehner, C. F. and O'Farrell, P. H. (1990). The roles of Drosophila cyclins A and B in mitotic control. *Cell* **61**, 535-547.
Leyns, L., Gómez-Skarmeta, J.-L. and Dambly-Chaudière, C. (1996). iroquois: a prepattern gene that controls the formation of bristles on the thorax of Drosophila. *Mech. Dev.* **59**, 63-72.
Martín-Blanco, E., Gampel, A., Ring, J., Virdee, K., Kirov, N., Tolkovsky, A. M. and Martinez-Arias, A. (1998). puckered encodes a phosphatase that mediates a feedback loop regulating JNK activity during dorsal closure in Drosophila. *Genes Dev.* **12**, 557-570.
Maurange, C. and Paro, R. (2002). A cellular memory module conveys epigenetic inheritance of hedgehog expression during Drosophila wing imaginal disc development. *Genes Dev.* **16**, 2672-2683.
McCusker, C. and Gardiner, D. M. (2011). The axolotl model for regeneration and aging research: a mini-review. *Gerontology* **57**, 565-571.
Mohan, M., Herz, H.-M., Smith, E. R., Zhang, Y., Jackson, J., Washburn, M. P., Florens, L., Eissenberg, J. C. and Shilatifard, A. (2011). The COMPASS family of H3K4 methylases in Drosophila. *Mol. Cell. Biol.* **31**, 4310-4318.
Mummery-Widmer, J. L., Yamazaki, M., Stoeger, T., Novatchkova, M., Bhalerao, S., Chen, D., Dietzl, G., Dickson, B. J. and Knoblich, J. A. (2009). Genome-wide analysis of Notch signalling in Drosophila by transgenic RNAi. *Nature* **458**, 987-992.
Ng, M., Diaz-Benjumea, F. J. and Cohen, S. M. (1995). Nubbin encodes a POU-domain protein required for proximal-distal patterning in the Drosophila wing. *Development* **121**, 589-599.
Ni, J.-Q., Liu, L.-P., Binari, R., Hardy, R., Shim, H.-S., Cavallaro, A., Booker, M., Pfeiffer, B. D., Markstein, M., Wang, H. et al. (2009). A Drosophila resource of transgenic RNAi lines for neurogenetics. *Genetics* **182**, 1089-1100.
Oktaba, K., Gutiérrez, L., Gagneur, J., Girardot, C., Sengupta, A. K., Furlong, E. E. M. and Müller, J. (2008). Dynamic regulation by polycomb group protein complexes controls pattern formation and the cell cycle in Drosophila. *Dev. Cell* **15**, 877-889.
Parkin, C. A. and Burnet, B. (1986). Growth arrest of Drosophila melanogaster on erg-2 and erg-6 sterol mutant strains of Saccharomyces cerevisiae. *J. Insect. Physiol.* **32**, 463-471.
Perkins, K. K., Dailey, G. M. and Tjian, R. (1988). Novel Jun- and Fos-related proteins in Drosophila are functionally homologous to enhancer factor AP-1. *EMBO J.* **7**, 4265-4273.
Richardson, H. E. H., O'Keefe, L. V. L., Reed, S. I. S. and Saint, R. R. (1993). A Drosophila G1-specific cyclin E homolog exhibits different modes of expression during embryogenesis. *Development* **119**, 673-690.
Riesgo-Escovar, J. R., Jenni, M., Fritz, A. and Hafen, E. (1996). The Drosophila Jun-N-terminal kinase is required for cell morphogenesis but not for DJun-dependent cell fate specification in the eye. *Genes Dev.* **10**, 2759-2768.
Ring, J. M. and Martinez Arias, A. (1993). puckered, a gene involved in position-specific cell differentiation in the dorsal epidermis of the Drosophila larva. *Dev. Suppl.* 251-259.
Rudenko, A., Bennett, D. and Alphey, L. (2003). Trithorax interacts with type 1 serine/threonine protein phosphatase in Drosophila. *EMBO Rep.* **4**, 59-63.
Ryder, E., Ashburner, M., Bautista-Llacer, R., Drummond, J., Webster, J., Johnson, G., Morley, T., Chan, Y. S., Blows, F., Coulson, D. et al. (2007). The DrosDel deletion collection: a Drosophila genomewide chromosomal deficiency resource. *Genetics* **177**, 615-629.
Sato, A. and Tomlinson, A. (2007). Dorsal-ventral midline signaling in the developing Drosophila eye. *Development* **134**, 659-667.
Schubiger, M., Sustar, A. and Schubiger, G. (2010). Regeneration and transdetermination: the role of wingless and its regulation. *Dev. Biol.* **347**, 315-324.
Schüpbach, T. and Wieschaus, E. (1991). Female sterile mutations on the second chromosome of Drosophila melanogaster. II. Mutations blocking oogenesis or altering egg morphology. *Genetics* **129**, 1119-1136.
Sluss, H. K., Han, Z., Barrett, T., Davis, R. J. and Ip, Y. T. (1996). A JNK signal transduction pathway that mediates morphogenesis and an immune response in Drosophila. *Genes Dev.* **10**, 2745-2758.
Smith-Bolton, R. K., Worley, M. I., Kanda, H. and Hariharan, I. K. (2009). Regenerative growth in Drosophila imaginal discs is regulated by Wingless and Myc. *Dev. Cell* **16**, 797-809.
Stewart, S., Tsun, Z.-Y. and Izpisua Belmonte, J. C. (2009). A histone demethylase is necessary for regeneration in zebrafish. *Proc. Natl. Acad. Sci. USA* **106**, 19889-19894.
Tapon, N., Harvey, K. F., Bell, D. W., Wahrer, D. C. R., Schiripo, T. A., Haber, D. A. and Hariharan, I. K. (2002). salvador Promotes both cell cycle exit and apoptosis in Drosophila and is mutated in human cancer cell lines. *Cell* **110**, 467-478.
Tie, F., Banerjee, R., Saiakhova, A. R., Howard, B., Monteith, K. E., Scacheri, P. C., Cosgrove, M. S. and Harte, P. J. (2014). Trithorax monomethylates histone H3K4 and interacts directly with CBP to promote H3K27 acetylation and antagonize Polycomb silencing. *Development* **141**, 1129-1139.
Tseng, A.-S., Carneiro, K., Lemire, J. M. and Levin, M. (2011). HDAC Activity Is Required during Xenopus Tail Regeneration. *PLoS ONE* **6**, e26382.
Tso, J. Y., Sun, X. H. and Wu, R. (1985). Structure of two unlinked Drosophila melanogaster glyceraldehyde-3-phosphate dehydrogenase genes. *CORD Conf. Proc.* **260**, 8220-8228.
Wang, L., Jahren, N., Miller, E. L., Ketel, C. S., Mallin, D. R. and Simon, J. A. (2010). Comparative analysis of chromatin binding by Sex Comb on Midleg (SCM) and other polycomb group repressors at a Drosophila Hox gene. *Mol. Cell. Biol.* **30**, 2584-2593.
Weng, M., Golden, K. L. and Lee, C.-Y. (2010). dFezf/Earmuff maintains the restricted developmental potential of intermediate neural progenitors in Drosophila. *Dev. Cell* **18**, 126-135.
White, R. A. H. and Wilcox, M. (1984). Protein products of the bithorax complex in Drosophila. *Cell* **39**, 163-171.
Worley, M. I., Setiawan, L. and Hariharan, I. K. (2012). Regeneration and transdetermination in drosophila imaginal discs. *Annu. Rev. Genet.* **46**, 289-310.
Wu, J. and Cohen, S. M. (2002). Repression of Teashirt marks the initiation of wing development. *Development* **129**, 2411-2418.
Xiong, Y., Li, W., Shang, C., Chen, R. M., Han, P., Yang, J., Stankunas, K., Wu, B., Pan, M., Zhou, B. et al. (2013). Brg1 governs a positive feedback circuit in the hair follicle for tissue regeneration and repair. *Dev. Cell* **25**, 169-181.

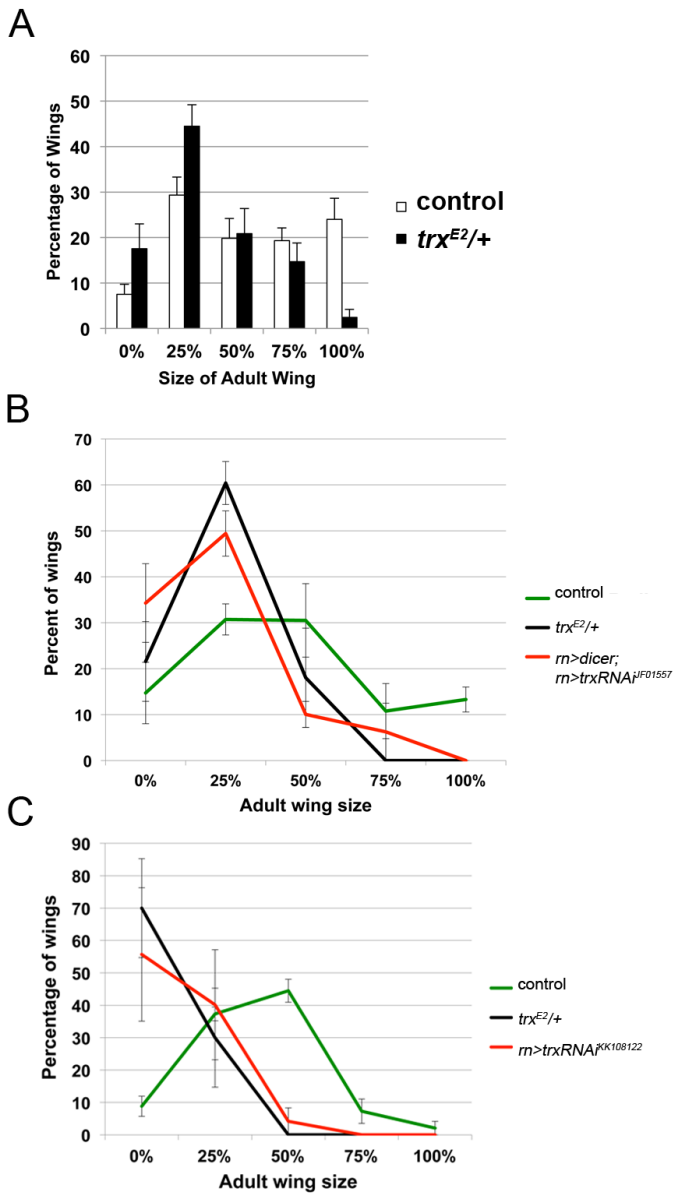

Figure S1. Reduction of *trx* is consistent across experiments. Regeneration experiments carried out in different seasons are affected by weather, humidity and food quality. Despite these changes trx^{E2}/+ wing discs do not regenerate as well as control wing discs. Figure 1H was the original experiment, with three independent replicates carried out over three months in the fall. A) 6 independent replicates carried out over 3 months in the summer, trx^{E2}/+ n=215, control n=456. Error bars are s.e.m. The distributions are significantly different, chi-squared test, $p<0.0001$. B-C) Regeneration as assessed by adult wing size using a line graph to facilitate comparing multiple genotypes, comparing trx^{E2}/+ and control animals to RNAi lines JF01557 (B) and KK108122 (C). Distributions of wing sizes for all mutants and RNAi lines were significantly different than the controls, chi-squared test $p<0.01$. 3 independent experiments each, for (B) control n=233 wings, trx^{E2}/+ n=128 wings, JF01557 n=82 wings; for (C) control n=157 wings, trx^{E2}/+ n=24 wings, KK108122 n=48 wings. Error bars are s.e.m.

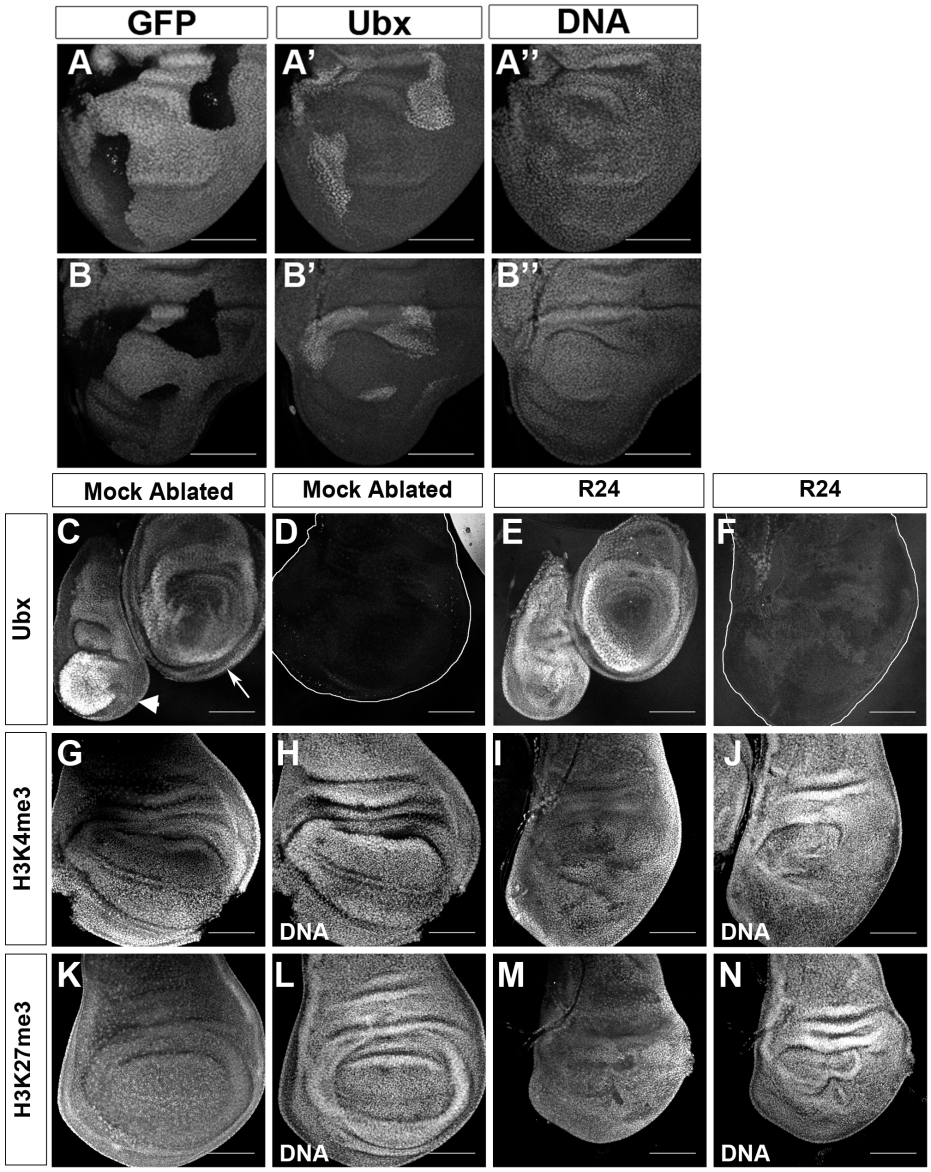

Figure S2. Tissue damage does not induce expression of *ubx* or broad changes in Histone methylation.

Homozygous mutant clones of *Scm*^{D1} in a *Minute*/+ background are marked by lack of GFP (A, B). Ubx is ectopically expressed within these clones (A', B'). TO-PRO3 staining shows DNA (A'', B''). See materials and methods for full genotypes. Scale bars are 100 micrometers. Anti-Ubx staining in C) haltere (arrowhead) and leg (arrow) discs from mock-ablated animals, D) mock-ablated wing disc, E) haltere and leg discs at R24 and F) wing disc at R24. Note slightly higher background in E and F, but absence of immunostaining in F. Two independent experiments, n=46 regenerating wing discs imaged at R0, R24 or R48 with no anti-Ubx staining. H3K4me3 antibody staining in a mock-ablated (G) and R24 (I) wing discs. DNA (TO-PRO3) shown for comparison (H,J). Three independent experiments, n=38 regenerating discs imaged at R0 or R24. H3K27me3 antibody staining in a mock-ablated (K) and R24 (M) wing discs. DNA (TO-PRO3) shown for comparison (L,N). Three independent experiments, n=22 regenerating discs imaged at R0 or R24.

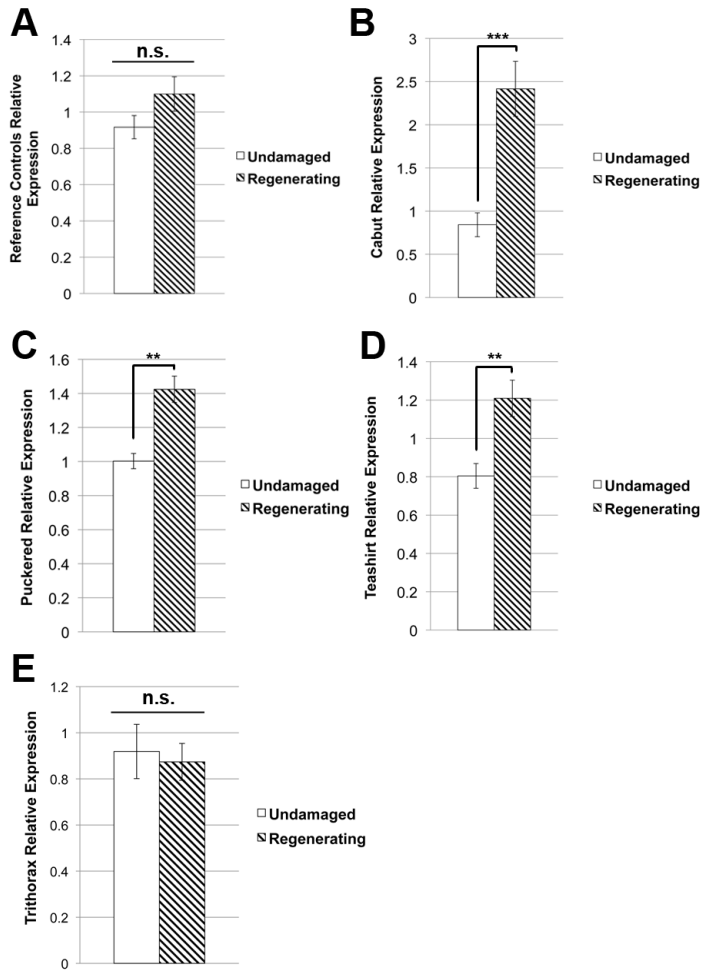

Figure S3. Analysis of gene expression changes in regenerating wing discs.
qRT-PCR of mock ablated and regenerating wing discs. A) Relative expression levels of *CG12703* compared to *gapdh2* showing no significant difference (n.s.) (p=0.22), making them useful reference controls. B) Relative expression levels of *cabut* compared to *gapdh2*, showing the ability to identify increased expression of a known regeneration gene. ***p=0.000074. C) Relative expression levels of *puckered* compared to *gapdh2*, showing the ability to detect elevation of JNK signaling in the blastema. **p=0.001. D) Relative expression levels of *teashirt* compared to *gapdh2*, showing increased representation of non-wing pouch cells. **p=0.0074. Error bars are SEM. E) Relative expression levels of *trx* compared to *gapdh2*, showing no significant changes in *trx* expression after tissue damage (n.s., p=0.61). Error bars are s.e.m. n was between 5 and 8 independent samples for all panels. Each sample was approximately 15 imaginal discs.

A

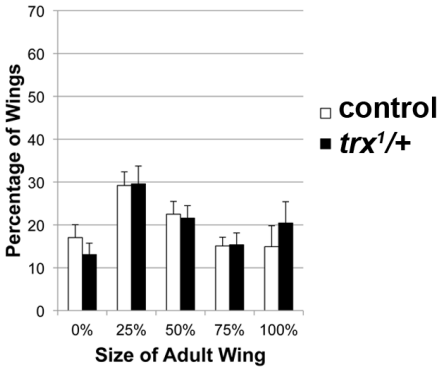

B

genotype	% of progeny	% of halteres transformed
ED5644/trxE2	0	na
ED5644/trx1	21	42
trxE2/trx1	41	32

Figure S4. An allelic series of *trx* mutants.
We compared animals trans-heterozygous for the deletion Df(3R)ED5644 or trx^{E2}, and the weak hypomorph trx^{1} (Ingham and Whittle, 1980), which is a 9 kb insertion in the first intron and results in a reduction in expression but not impairment of the protein (Breen, 1999). A) Animals heterozygous for trx^{1} had no regeneration phenotype. Three independent experiments. trx^{1} n=181 wings, control n=296 wings. Error bars are s.e.m. The distributions of wings sizes are not significantly different, chi-squared test p=0.188. B) Percentage of progeny that were trans-heterozygous mutant after crossing two balanced alleles together. Progeny with both balancers were not viable. n=209, 155, and 75 total progeny for the three crosses depicted. Percentage of halteres that had partially or completely transformed to wings in the given genotypes. n=64 and 62 halteres for the genotypes depicted. Note that trx^{1} was viable in combination with *Df(3R) ED5644* or trx^{E2} . These trans-heterozygous combinations showed different percentages of viable adults, suggesting that trx^{E2} is a slightly weaker allele than the deletion. Examination of trans-heterozygous adults revealed an increased frequency of haltere-to-wing transformations (Rudenko et al., 2003) in the *Df(3R)ED5644* / trx^{1} animals compared to the trx^{E2} / trx^{1} animals, again suggesting an allelic series in which *Df(3R)ED5644* is a stronger allele than trx^{E2}, which is significantly stronger than trx^{1}.

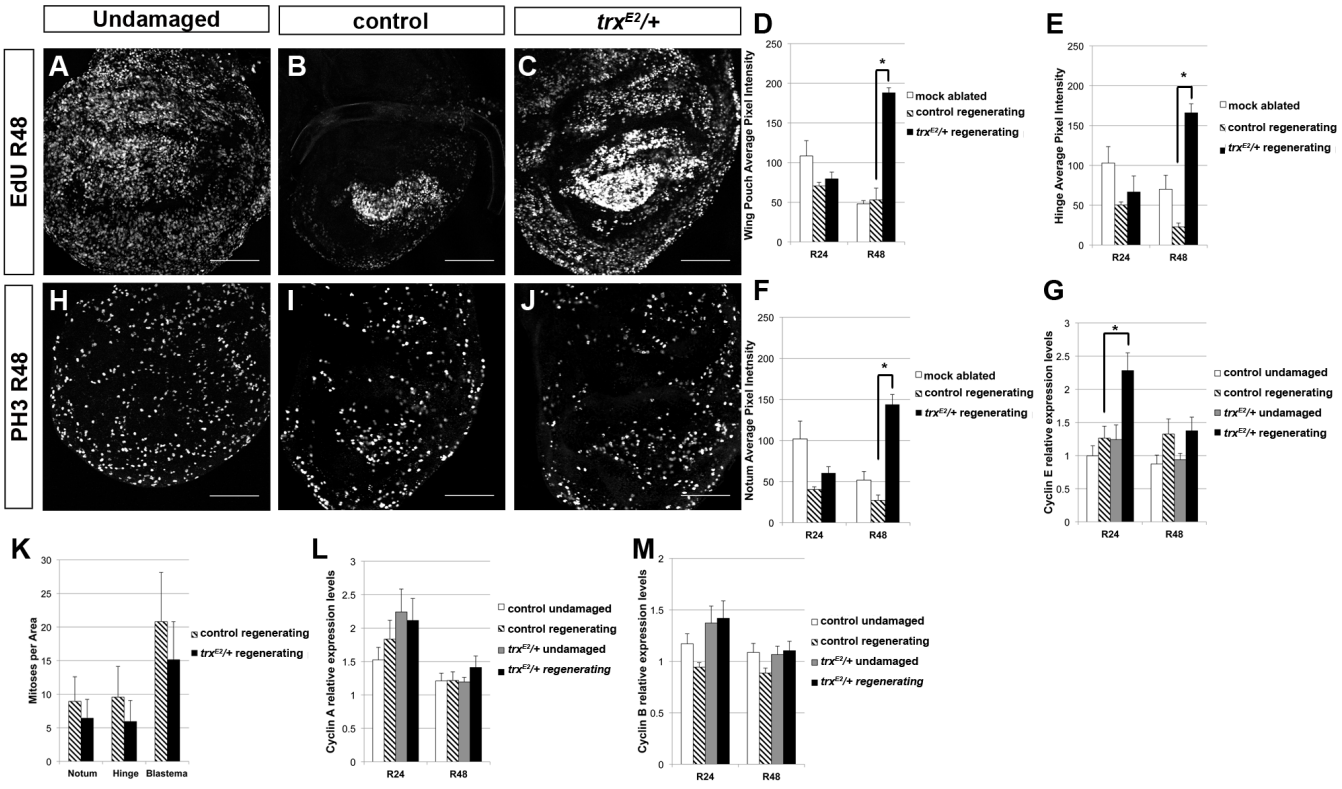

Figure S5. The cell cycle in control and mutant regenerating discs.
A-C) Representative examples of EdU incorporation marking cells in S phase in mock-ablated (A), as well as regenerating control (B) and *trx*^{E2}/+ (C) imaginal wing discs at R48. Similar results were obtained in 3 independent experiments. Quantification of average pixel intensity in the wing pouch (D), hinge (E) and notum (F) regions of the wing disc at the same time points. Regions of interest were identified by morphological features and Nubbin immunostaining. n was between 4 and 19 discs per genotype per time point from two independent replicates. G) qRT-PCR quantification of *cyclinE* expression in undamaged and regenerating wing discs at R24 and R48. n was between 5 and 8 independent samples per genotype per time point. H-J) Representative examples of PH3 immunostaining in mitotic cells in mock-ablated (H), as well as regenerating control (I) and *trx*^{E2}/+ (J) imaginal wing discs at R48. Similar results were obtained in 3 independent experiments. K) Quantification of mitotic cells per area in the wing pouch at R48. n was between 12 and 16 discs per genotype and time point from two independent replicates. p>0.2 in the blastema, indicating minimal difference in mitotic rates as the animals entered pupariation. L-M) qRT-PCR quantification of *cyclinA* and *cyclinB* expression in mock ablated and regenerating wing discs at R24 and R48. n was between 5 and 8 independent samples per genotype and time point. Differences between *trx*^{E2}/+ regenerating discs and all other samples were not statistically significant. Error bars in D, E, F, G, L and M show s.e.m. Error bars in K shows s.d. Scale bars are 100 micrometers. * = $p<5x10^{-5}$ for D-G.

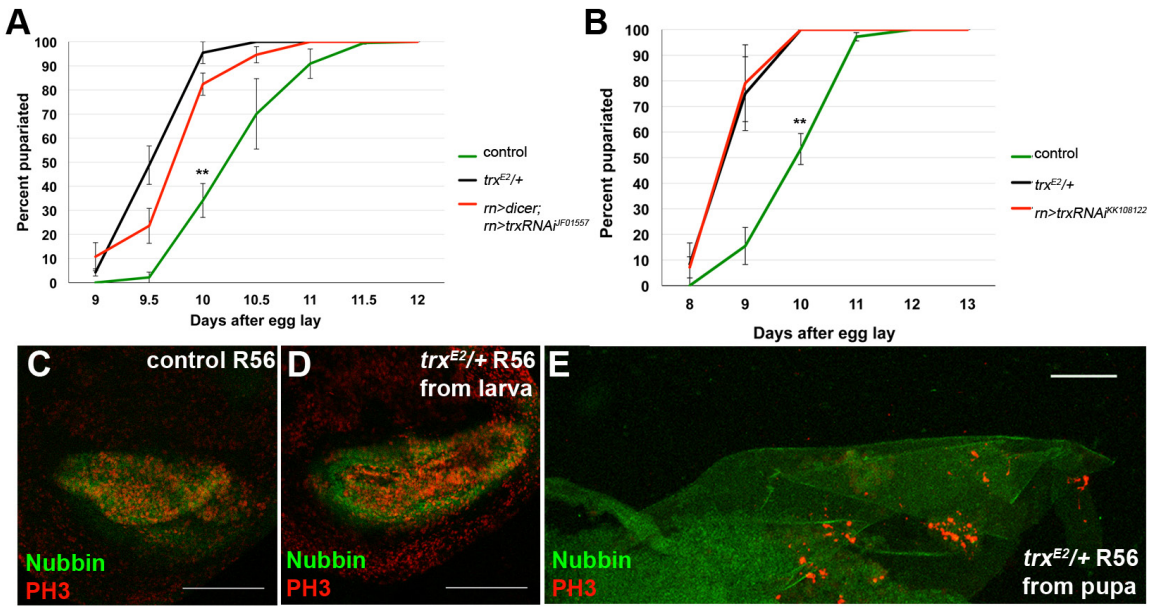

Figure S6. Pupariation stops regenerative growth. A-B) Pupariation rates, comparing *trx*^{E2}/+ and control animals to RNAi lines JF01557 (A)(**p<5x10^{-4} at day 10) and KK108122 (B) (**p<0.01 at day 10). 3 independent experiments each, for (A) control n=123, *trx*^{E2}/+ n=58, JF01557 n=26; for (B) control n=135, *trx*^{E2}/+ n=12, KK108122 n=29. C-E) Wing discs stained for Nubbin (green) and PH3 (red). Error bars are s.d. C) Representative control larval wing disc at R56. D) *trx*^{E2}/+ larval wing disc at R56. Disc was from the only remaining larva; all other *trx*^{E2}/+ animals had pupariated at R56. E) *trx*^{E2}/+ pupal wing disc at R56. Most pupal *trx*^{E2}/+ discs were small and folded. Note the near absence of PH3 staining in the pupal *trx*^{E2}/+ R56 disc compared to the larval *trx*^{E2}/+ and control R56 discs. Scale bars are 100 micrometers.

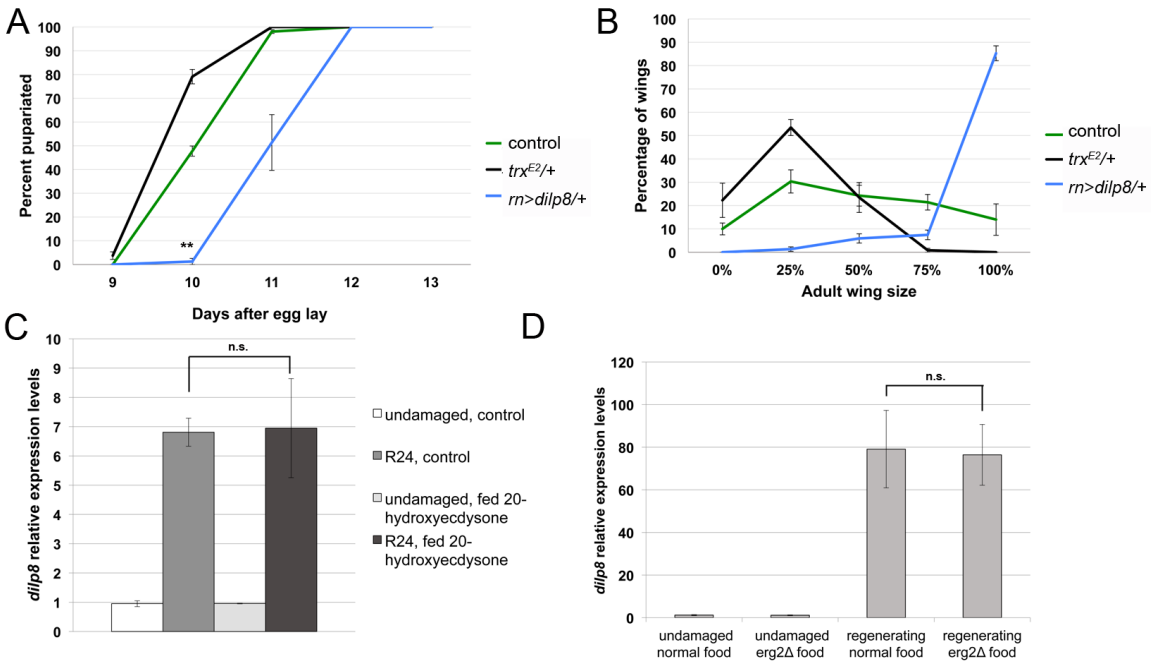

Figure S7. Pupariation and regeneration after overexpression of *dilp8*. A) Pupariation rates in control, trx^{E2}/+, and *rn>dilp8*/+ regenerating animals. Note that *dilp8* overexpression in the *rn*-expressing cells during the thermal shift is sufficient to delay pupariation longer than controls, **$p<10^{-7}$ on day 10. 5 independent experiments, control n=123, trx^{E2}/+ n=81, *rn>dilp8*/+ n=130. Error bars are s.e.m. B) Adult wing size as a measure of extent of regeneration in control, trx^{E2}/+, and *rn>dilp8*/+ animals. Note that the extended time before pupariation in the *rn>dilp8*/+ regenerating animals enabled enhanced regeneration, chi-squared test $p<5x10^{-50}$. 5 independent experiments, control n=180 wings, trx^{E2}/+ n=126 wings, *rn>dilp8*/+ n=273 wings. Error bars are s.e.m. C) *dilp8* relative expression levels as measured by qRT-PCR in undamaged and R24 regenerating discs from larvae that were fed 20-hydroxyecdysone from R6 to R24. Note that *dilp8* expression was unchanged by feeding 20-hydroxyecdysone, n.s. = not significantly different. 3 or 4 independent samples were used per condition. Error bars are s.d. D) *dilp8* relative expression levels as measured by qRT-PCR in undamaged and regenerating discs from larvae that were fed normal food and *erg2Δ* yeast food. Note that *dilp8* expression was unchanged when ecdysone production was limited, n.s. = not significantly different. Two independent samples were used for the undamaged discs, and 4 or 5 independent samples were used for the regenerating discs. Error bars are s.d.

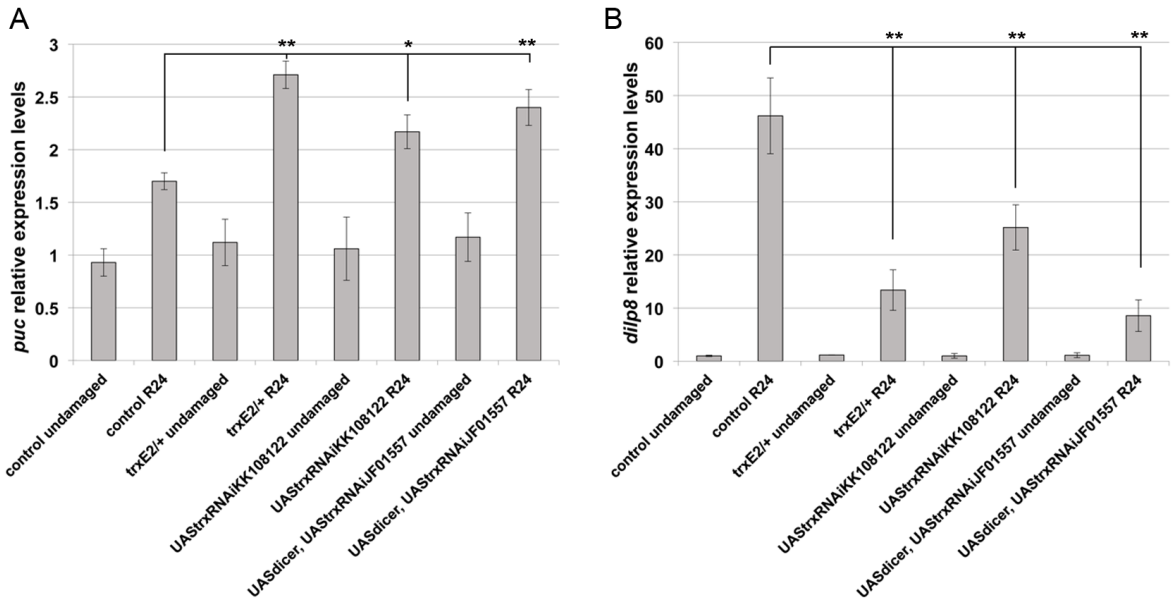

Figure S8. Knockdown of Trx via RNAi phenocopies the heterozygous mutant phenotype. A) *puc* relative expression determined by qRT-PCR in undamaged and R24 wing discs of the noted genotypes. Reducing *trx* levels increased *puc* expression at R24, *p<0.2, **p<10^{-5}. 3 or 4 independent samples for each genotype and condition. Error bars are s.d. B) *dilp8* relative expression determined by qRT-PCR in undamaged and R24 wing discs of the noted gentypes. Reducing *trx* levels decreased *dilp8* expression at R24, **p<0.005. 3 or 4 independent samples for each genotype and condition. Error bars are s.d.

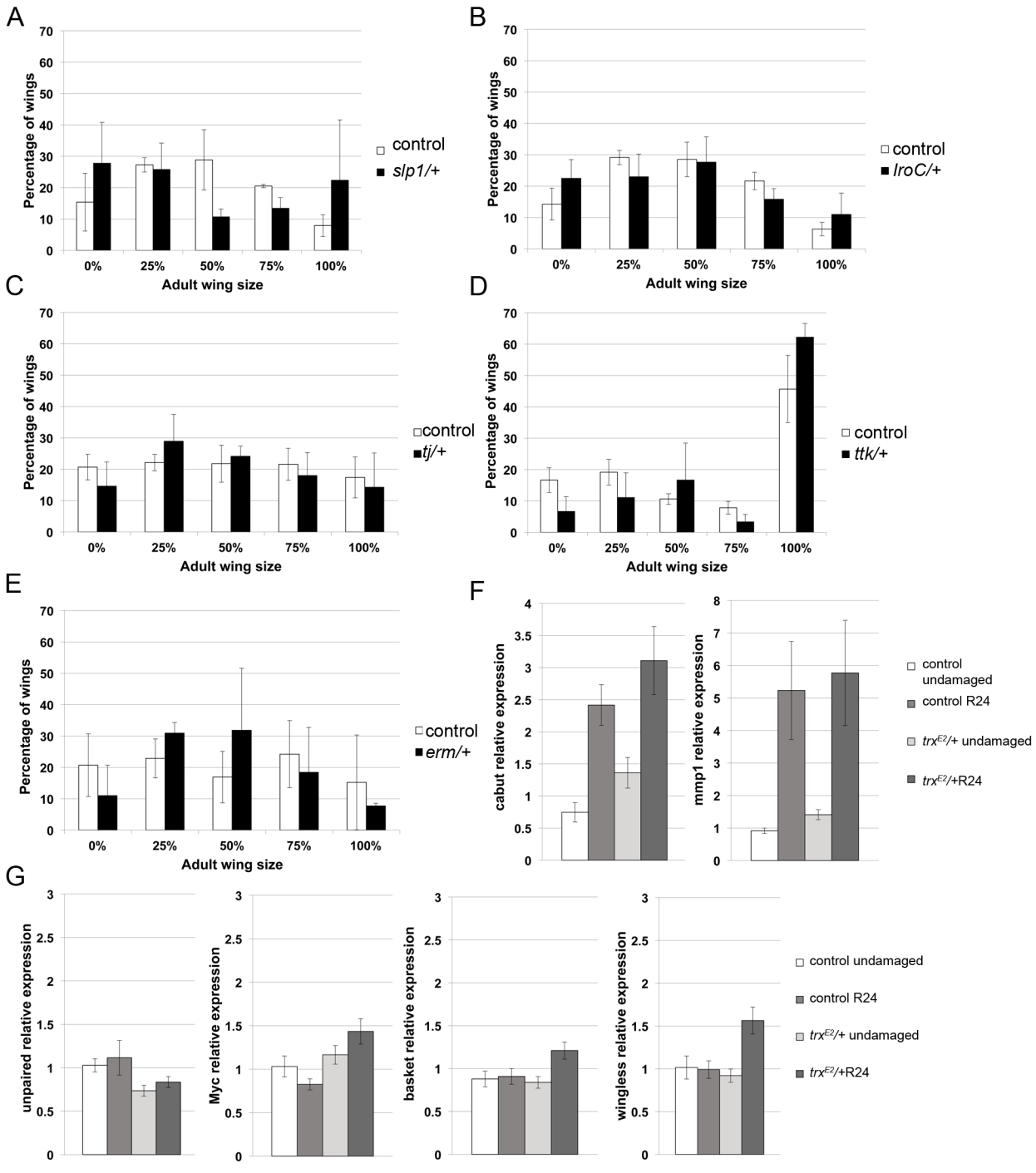

Figure S9. Candidate *trx* targets that do not affect regeneration or are not reduced in *trx*^{E2}/+ regenerating wing discs. A-E) Ablation and regeneration were induced in the wing imaginal discs. Adult wings were sorted by size to quantify extent of regeneration. None of the genotypes tested regenerated worse than controls. Differences among experiments are due to changes in food and humidity. All error bars are s.e.m., except for *erm*/+, which is s.d. A) *sloppy-*

paired 1 (slp1). Three independent experiments, control n=100 $slp1^{05965}$/+ n=150. B) *Iroquois Complex (IroC)*. Five independent experiments, control n=210, $IroC^{DNF2}$/+ n=90. C) *traffic jam (tj)*. Three independent experiments, control n=168, tj^{PL3}/+ n=64. D) *tramtrack (ttk)*. Three independent experiments, control n=247, ttk^{rM730}/+ n=58. E) *earmuff (erm)*. Two independent experiments, control n=76, erm^{f07652}/+ n=52. F-G) Relative expression levels of regeneration genes were quantified by qRT-PCR in undamaged and R24 wing imaginal discs. Between 4 and 8 independent samples per genotype and condition. All error bars are s.e.m. F) Relative expression levels of regeneration genes *cabut* and *mmp1* are not reduced in trx^{E2}/+ wing discs. G) Relative expression levels of regeneration genes *unpaired*, *myc*, *basket*, and *wingless* are not reduced in trx^{E2}/+ wing discs.

Gene	Forward Primer Sequence (5'-3')	Reverse primer sequence (5'-3')	Source
basket	CGCCACTTTGAGTGCCCAGTGT	GAGCAAGGAGCATATCGGCCATTTA	
cabut	AAGCGCCAGTGCAAAGTTAGCTG	TTGTTCGTCCTTGGCGACGATTTC	
CG12703			(Classen et al., 2009)
Cyclin A	AAGATGCATATCAGGTCTTCCGTGA	GCTCCTTCTGCCCAGCACCG	
Cyclin B	TGACAATCCCGCACTCGACTTG	AAGCGTTCTCATCGCCACGCA	
Cyclin E	ACGACGACGACGAAAAACTCTCG	GCTGGTAGAACAAACACTCTTGGCA	
dilp8			Qiagen QT00510552
E74			Qiagen QT00510874
GAPDH2			(Classen et al., 2009)
lacZ			(Hatton et al., 2000)
mmp1	TCGGCTGCAAGAACACGCCC	CGCCCACGGCTGCGTCAAAG	
myc	CAACTTGCTGGCGGCACGG	TCCTGAGTTATATGCCTGTCTCGCT	
puckered	GTCCTAGCAATCCTTCGTCATC	ATCATCGTAATCAAACCCATCC	
teashirt	AGGGGTAAAAGCTCCAGAAGAA	GCTCAATGGCACTTAAAACAGA	
trithorax			Qiagen QT00974589
unpaired	AGCGTCCCAGGCAGAGCTTCA	TACTCCCGAAAGGCGTGGCG	
wingless	CTCCTCCGCTCGAAACGCCG	TCCGCTGGATCACACGGCAA	

Table S1. Primers used for qRT-PCR or PCR. Primer sequences, references containing primer sequences, or sources for commercially available primers used for qRT-PCR or PCR.

Supplemental methods

Fly lines and genetics

Fly lines obtained from the Bloomington Stock Center were Df(3R)ED5644, Df(3R)ED6346, Df(3R)ED5147 and Df(3R)ED5230 (Ryder et al., 2007), *trx*^{E2} (Kennison and Tamkun, 1988), *trx*^{1} (Ingham and Whittle, 1980), *puc*^{e69} (JM and A, 1993), and *bsk*^{1} (Riesgo-Escovar et al., 1996), *ttk*^{rn730} which reduces expression of both Ttk88 and Ttk69 (Lai and Li, 1999), *erm*^{f07652}, *tj*^{PL3} (Schüpbach and Wieschaus, 1991), *slp1*^{05965} (Sato and Tomlinson, 2007), and *iro*^{DFM2} which removes *ara* and *caup* (Leyns et al., 1996) Additional lines used were *rn-GAL4*, *UAS-reaper*, *tub-GAL80*^{TS} / *TM6B GAL80* (Smith-Bolton et al., 2009), *w*^{1118} (Hazelrigg et al., 1984), *UAS-puc* obtained from FlyORF (University of Zurich) (Bischof et al., 2013), *UAS-dilp8* (gift of M. Dominguez, Universidad Miguel Hernandez) (Garelli et al., 2012), *UAStrxRNAi*^{JF01557} (TRiP)(Ni et al., 2009), *UAStrxRNAi*^{KK108122} (VDRC)(Dietzl et al., 2007), and the AP-1 reporter TRE-red (gift of Dirk Bohmann, University of Rochester) (Chatterjee and Bohmann, 2012). Mitotic clones of *Scm* mutant tissue were generated in a Minute background by crossing *y,w,hsFLP; FRT82B ubi-GFPnls RpS3[Plac92]* / *TM6B* to *w; FRT82B, Scm*^{D1} / *TM6C, Sb, Tb* and heat shocking to induce recombination.

Immunohistochemistry

Primary antibodies were anti-β-Galactosidase (1:500) (Cappel, MP Biomedicals), anti-Ubx (1:500) (White and Wilcox, 1984), anti-H3K4me3 (1:500) (Active Motif), anti-H3K27me3 (1:200) (Active Motif), anti-PH3 (1:500) (Millipore), anti-Nubbin (1:100) (a gift of Steven Cohen, National University of Singapore) (Ng et al., 1995), anti-cleaved Caspase 3 (1:200) (Cell Signaling, lot # 18), anti-Wingless (1:50) (Brook and Cohen, 1996), anti-phospho-JNK (1:100 for 4 days at 4°C blocking with 1% BSA and 10% Normal Goat Serum in Tris-buffered saline with 0.1% Triton X-100) (Santa Cruz Biotechnology). The anti-Ubx and anti-Wingless antibodies were obtained from the Developmental Studies Hybridoma Bank developed under the auspices of the NICHD and maintained by The University of Iowa, Department of Biology, Iowa City, IA 52242. Discs were mounted in Vectashield mounting medium (Vector Laboratories).

Secondary antibodies were AlexaFluor probes (488, 555, 633) (1:1000) (Life Technologies). DNA was marked using TO-PRO3 (1:500) (Life Technologies) or DAPI (1:5000 of 0.5 mg/mL stock) (Sigma).

EdU incorporation was carried out as previously described (Gouge and Christensen, 2010) using the Click-It EdU kit (Life Technologies). Tissue was incubated in EdU for 20 minutes at room temperature.

Imaging Analysis

All quantified images used the same imaging parameters within a given experiment. EdU incorporation was quantified by measuring the average pixel intensity within the Nubbin-positive region or in 100 x 100 pixel boxes of projected z-stacks using ImageJ, three boxes per region per disc. Mitosis rates in projected z-stacks were quantified by counting the number of PH3-positive nuclei in 100 x 100 pixel boxes within the Nubbin-positive region, the notum, or the hinge, three boxes per region per disc. The size of the wing pouch was quantified by counting the

number of pixels in the Nubbin-positive area using ImageJ. The AP-1 reporter and phospho-JNK immunostaining were quantified by measuring average pixel intensity in the Wingless-positive or Nubbin-positive region of the disc in a single confocal slice using ImageJ.